A Journal of the Gesellschaft Deutscher Chemiker

Angewandte International Edition GDCh Chemie

www.angewandte.org

## Accepted Article

**Title:** Hydrazone-Linked Covalent Organic Frameworks

**Authors:** Huifen Zhuang, Can Guo, Jianlin Huang, Liwen Wang, Zixi Zheng, Hai-Ning Wang, Yifa Chen, and Ya-Qian Lan



**To be cited as:** *Angew. Chem. Int. Ed.* **2024**, e202404941

**Link to VoR:** https://doi.org/10.1002/anie.202404941

WILEY VCH

10.1002/anie.202404941

WILEY-VCH

REVIEW

# Hydrazone-Linked Covalent Organic Frameworks

Huifen Zhuang,[a]‡ Can Guo,[a]‡ Jianlin Huang,[a]‡ Liwen Wang,[a] Zixi Zheng,[a] Hai-Ning Wang,*[b] Yifa Chen,*[a] and Ya-Qian Lan*[a]

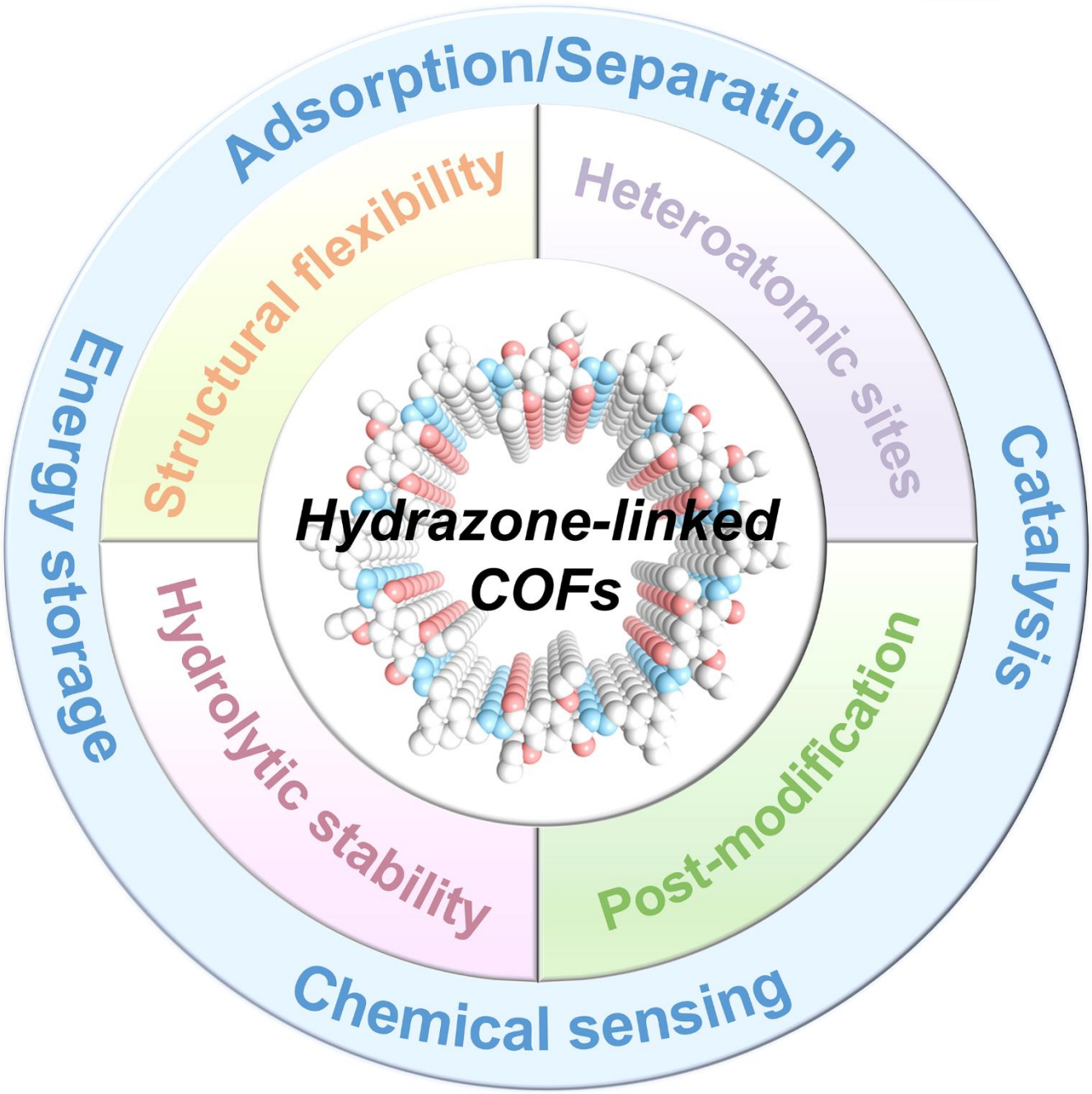

10.1002/anie.202404941

WILEY-VCH

REVIEW

[a] H. Z., C. G., J. H., L. W, Z. Z., Prof. Y. C., Prof. S.-L. L. and Prof. Y.-Q. L.
School of Chemistry
South China Normal University
Guangzhou, 510006, P. R. China
E-mail: chyf927821@163.com; yqlan@m.scnu.edu.cn
[b] H. W.
School of Chemistry and Chemical Engineering
Shandong University of Technology
Zibo, 255049, P. R. China
E-mail: wanghn913@foxmail.com

**Abstract:** Hydrazone-linked covalent organic frameworks (COFs) with structural flexibility, heteroatomic sites, post-modification ability and high hydrolytic stability have attracted great attention from scientific community. Hydrazone-linked COFs, as a subclass of Schiff-base COFs, was firstly reported in 2011 by Yaghi's group and later witnessed prosperous development in various aspects. Their adjustable structures, precise pore channels and plentiful heteroatomic sites of hydrazone-linked structures possess much potential in diverse applications, for example, adsorption/separation, chemical sensing, catalysis and energy storage, etc. Up to date, the systematic reviews about the reported hydrazone-linked COFs are still rare. Therefore, in this review, we will summarize their preparation methods, characteristics and related applications, and discuss the opportunity or challenge of hydrazone-linked COFs. We hope this review could provide new insights about hydrazone-linked COFs for exploring more appealing functions or applications.

## 1. Introduction

Covalent organic frameworks (COFs), representing as a big family of porous organic polymers constructed via covalent connection of organic ligands, have attracted giant attention of scientists around the world.[1] They display unique structural merits, such as rigid skeletons, high surface area and good crystallinity, which makes them attractive for applications in adsorption/separation, catalysis, chemical sensing, energy storage, etc.[2] Since 2005, scientists have been constantly seeking to develop COFs with novel structures and functions. Thanks to the state-of-the-art synthetic technology, a multitude types of dynamic covalent bonds have been synthesized with distinctive structures, enriching the diversity of COFs family (Figure 1).[3] Schiff-base COFs, are a large class of COFs with the most studied and reported works due to their advantages of high chemical stability, abundantly accessible ligands and reversible bonding reaction, etc.[3d,3e,3h,3j,4] Among the reported Schiff-base COFs, hydrazone-linked COFs as an important subclass was firstly reported in 2011 by Yaghi's group.[3i] Later, the hydrazone-linked COFs have drawn more and more interest because of their unique characteristics, functions and properties. In view of their prosperous development and increasing importance in various aspects, we intend to present a brief summary of hydrazone-linked COFs at the current stage, hoping to attract more and more scientists to contribute to such a rising star of COFs.

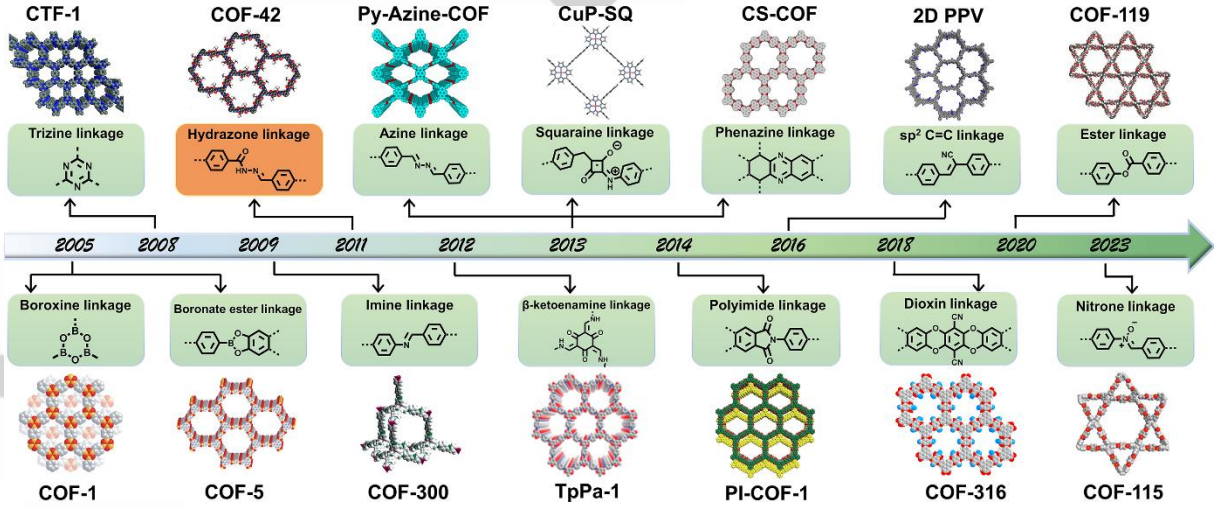


***Figure 1.*** The development timeline of COFs with different linkages. Image for COF-1 and COF-5: Reproduced with permission.[3a] Copyright 2005, American Association for the Advancement of Science. Image for CTF-1: Reproduced with permission.[3f] Copyright 2008, Wiley-VCH. Image for COF-300: Reproduced with permission.[3i] Copyright 2008, American Chemical Society. Image for COF-42: Reproduced with permission.[3i] Copyright 2011, American Chemical Society. Image for Tapa-1: Reproduced with permission.[3e] Copyright 2012, American Chemical Society. Image for Py-Azine-COF: Reproduced with permission.[3b] Copyright 2013, American Chemical Society. Image for CuP-SQ-COF: Reproduced with permission.[3h] Copyright 2013, Wiley-VCH. Image for CS-COF: Reproduced with permission.[3d] Copyright 2013, Spring Nature. Image for PI-COF-1: Reproduced with permission.[3c] Copyright 2014, Spring Nature. Image for 2D PPV COF: Reproduced with permission.[3m] Copyright 2016, Royal Society of Chemistry. Image for COF-316: Reproduced with permission.[3k] Copyright 2018, American Chemical Society. Image for COF-119: Reproduced with permission.[3l] Copyright 2020, American Chemical Society. Image for COF-115: Reproduced with permission.[3g] Copyright 2023, Wiley-VCH.

10.1002/anie.202404941





Hydrazone linkage is a kind of unique bonding mode assigned to Schiff-base linkage, which would possess intrinsic functions that can inherit from Schiff-base linkage while novel properties by itself through a specific selection of structure struts. Compared with other Schiff-base linkage modes, hydrazone linkage displays the following advantages (Figure 2): 1) there existed changeable conformations for the hydrazone bond and the interconversion between each conformation mode would result in high structural flexibility;[5] 2) heteroatoms (i.e., N and O) in hydrazone bond would effectively induce the strong electrostatic interaction or electronegativity;[6] 3) the reactive activity of hydrazone linkage endows the structure with post-modification ability[7] and 4) the stable hydrazone linkage imparts the structure of hydrazone-linked COFs with high hydrolytic stability[8] when compared with traditional Schiff-base COFs (Figure 2).

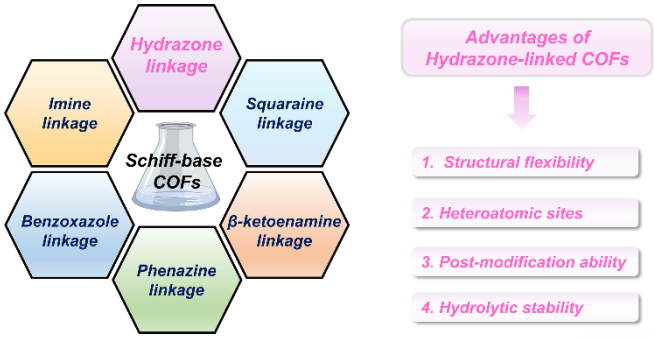


***Figure 2.*** Classification of Schiff-base COFs and advantages of hydrazone-linked COFs.

In this review, we will provide an exhaustive overview on the recent development of hydrazone-linked COFs including their design, preparation methods, characteristics, and applications (Figure 3). The following contents can be divided into four sections. Initially, we will present some basic information about hydrazone-linked COFs including their design, characteristics and preparation methods. After that, we will concentrate on the applications of hydrazone-linked COF, including adsorption/separation, catalysis, chemical sensing, and energy storage, and meanwhile discuss their structure-to-property relationships. Finally, we will present a perspective on their challenge and opportunity. We believe that this review will present a thorough and integrated explanation of the fundamental concepts, key applications, current bottlenecks and future development of hydrazone-linked COFs to trigger more and more interest in this field.


***Figure 3.*** The applications of hydrazone-linked COFs.

## 2. The characteristics and preparation methods

### 2.1. The characteristics of hydrazone-linked COFs

The design of hydrazone-linked COFs follows the principles of traditional Schiff-base reaction. In general, the formation mechanism of hydrazine linkage is based on the following reaction steps: initially, the amino group on the amino ligand functions as a nucleophile to interact with the carbonyl carbon of aldehyde ligand and undergo intramolecular proton transfer to generate intermediates, further leaving a displaced water molecule to form the hydrazone-linked COFs (Table 1). Based on the reaction mode, a large number of organic ligands have been selected for the building of hydrazone-linked COFs and the category of the reported organic ligands are summarized in Table 1.

Based on the reported organic ligands, hydrazone-linked COFs can be imparted with distinct features by specifically selecting structural struts, which can be designed to tune their structure and functionality. Up to date, different characteristics reported for hydrazone-linked COFs can be basically summarized: structural flexibility, heteroatomic sites, post-modification ability and hydrolytic stability, etc. (Figure 4). We will discuss these characteristics and present some representative examples to highlight the superiority of hydrazone-linked COFs in the following section.

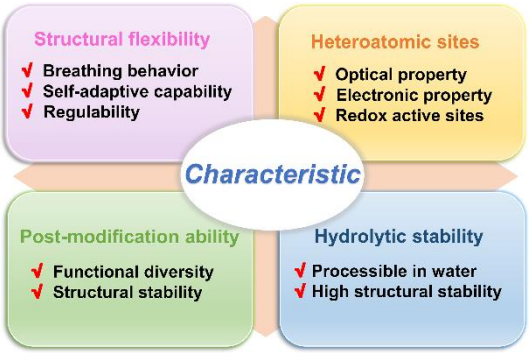


***Figure 4.*** Characteristics of hydrazone-linked COFs.

10.1002/anie.202404941



***Table 1.*** Reaction mechanism and some common ligands used for hydrazone-linked COFs.

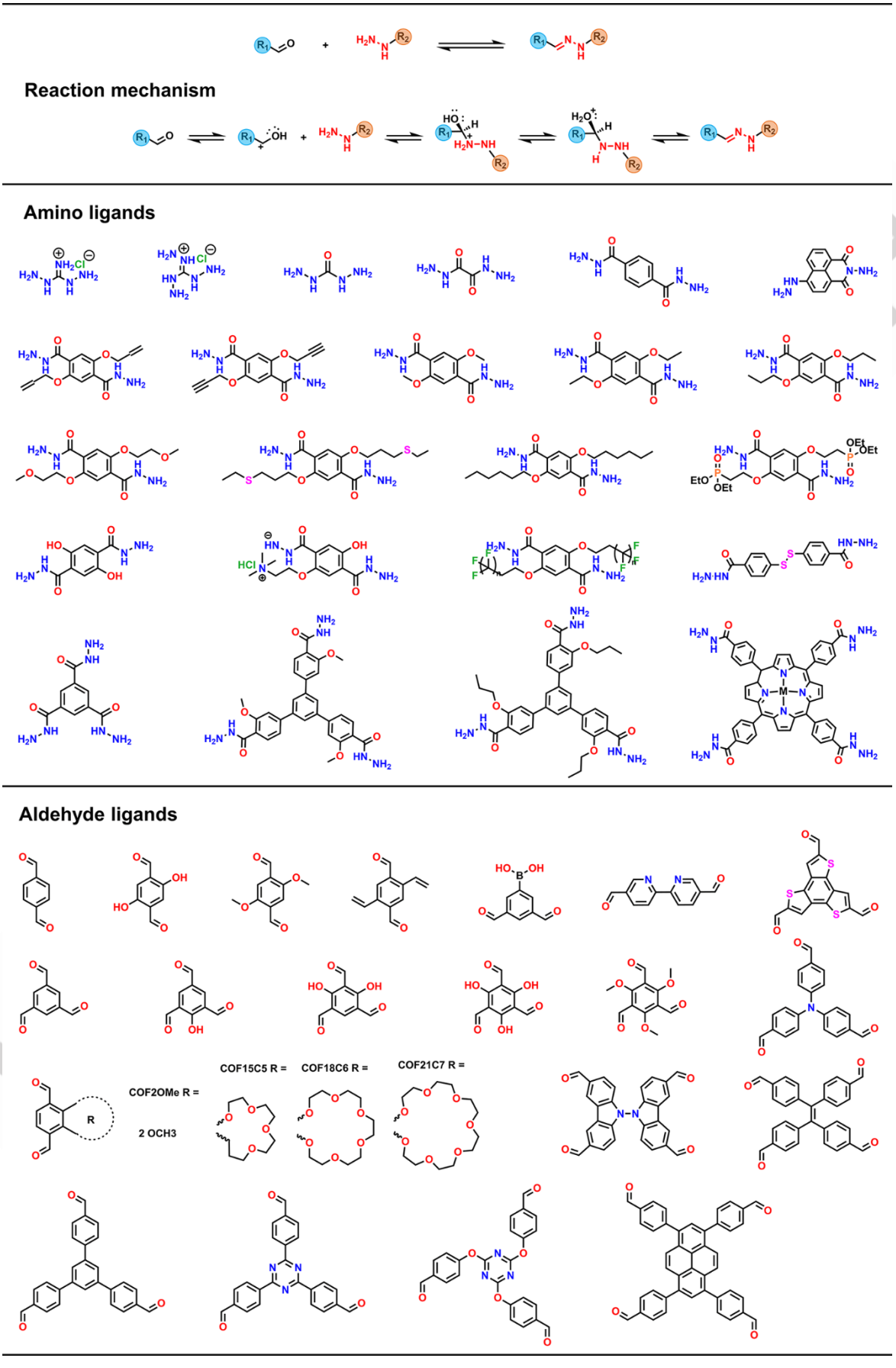

10.1002/anie.202404941





Huifen Zhuang received her B.S. degree at Guangzhou University in 2022, and is now studying for a postgraduate degree at South China Normal University under the supervision of Prof. Ya-Qian Lan and Prof. Yifa Chen. Her research interest focuses on the design and synthesis of COFs for energy-storage.

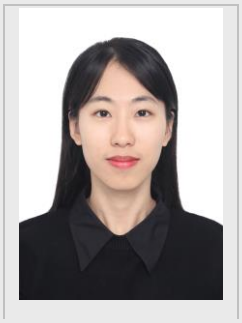

Can Guo received her M.S. degree at Jiangsu Normal University in·2019. Now she is a Ph.D. student in the School of Chemistry at South China Normal University, working under the supervision of Prof. Ya-Qian Lan and Prof. Yifa Chen. Her research interest focuses on the applications of porous crystalline materials in the energy-storage field.

Hai-Ning Wang received his BSc degree from Northeast Normal University in 2009, School of Chemistry, and in the same year, he joined Professor Zhong-Min Su to pursue his Ph.D. in physical chemistry from Northeast Normal University. In 2017, he carried out postdoctoral studies with Prof. Ya-Qian Lan in Inorganic Chemistry. Now, he is working at Shandong University of Technology. His research interests focus on the synthesis and properties of crystalline porous materials.

Yifa Chen received his B.S. degree from School of Chemistry, Beijing Institute of Technology. He subsequently obtained his Ph.D. degree from School of Chemistry and Chemical Engineering, Beijing Institute of Technology under the supervision of Prof. Bo Wang. In 2022, he joined South China Normal University (SCNU, China) as a professor of chemistry. His research interest focuses on the fabrication of porous crystalline material based devices like membranes, foams and fibers that can be applicable in energy storage, environment treatment or photo-/electro-catalysis.

Ya-Qian Lan received his B.S. and Ph.D. degrees (2009) from Northeast Normal University under the supervision of Prof. Zhong-Min Su. In 2010, he joined the National Institute of Advanced Industrial Science and Technology (AIST, Japan) as a JSPS postdoctoral fellow. In 2012, he became a professor of chemistry at Nanjing Normal University (NNU, China). In 2021, he joined South China Normal University (SCNU, China) as a professor of chemistry. His current research interest focuses on the synthesis of new crystalline materials and catalytic research related to clean energy applications.

### 2.1.1. Structural flexibility

In general, the structural flexibility would impart porous crystalline materials with more possibility in potentially extended functions and related applications.[9] However, the dilemma between crystallinity and structure of COFs set obstacles for achieving high flexibility in the structures. Specifically, hydrazone bond, a kind of flexible covalent bond formed by aldehyde ligand and hydrazide ligand, is relatively easier to construct when compared with traditional Schiff-base bonds and thus can permit structural flexibility to hydrazone-linked COFs. Due to the changeable conformations and certain elasticity of flexible hydrazone linkage, it has certain structural flexibility and can endow the hydrazone-linked COFs with advantages like breathing behavior, self-adaptive capability and regulability. For example, Zhao et al. realized the stepwise regulation of the flexibility of hydrazone-linked COFs (i.e., R-COF with rigid skeleton, SF-COF with semi-flexible skeleton and F-COF with flexible skeleton).[5c] Through response test toward tetrahydrofuran stimuli, the authors discovered that the F-COF exhibited obvious response to external stimuli, whereas the R-COF showed no response at all, which proved that COFs with varying degrees of flexibility would show distinct dynamic behaviors. Moreover, iodine ($I_2$) capture experiment was carried out to justify its self-adaptive capability. Interestingly, the higher $I_2$ adsorption capabilities were demonstrated by F-COF and SF-COF than by R-COF (at 383 K), which could be attributed to the self-adaptive ability of the flexible COFs through more expanded pores.

In addition to these two features (breathing behavior and self-adaptive capability), hydrazone-linked COFs also have regulablity. For example, in 2018, Li et al. regulated the flexibility of hydrazone-linked COFs (i.e., TFPB-DHzDAll, TFPB-DHzDPr, Tf-DHzDPr and Tf-DHzDAll) using a hydrogen-bonding-regulated strategy.[5a] There was no fluorescence in the initial hydrazone-linked COFs due to the free bond rotation. Interestingly, the introduction of intra- and inter-layer hydrogen bonding interactions into the COF structure can result in the restriction of the intramolecular bond and thus significantly enhance the fluorescence. It could be summarized that the degree of flexibility could be limited by intra- and interlayer hydrogen bonding, making hydrazone-linked COFs regulable. Along the same line, Jiang et al. thoroughly studied the flexibility of H-COFs with hydrazone linkage through the regulation of hydrogen bonding.[5b] Significantly, the observation of long-lived room-temperature phosphorescence was made possible by regulating the quantity

of intramolecular hydrogen bonds presented in the COFs, which might promote the development of room-temperature delayed fluorescence materials with COF structures.

#### 2.1.2. Heteroatomic sites

The introduction of heteroatomic sites into structure has become an effective tool for customizing COFs and improving the performance of COFs.[10] Hydrazone-linked COFs contain abundant N and O sites could generate supramolecular forces such as intra-/interlayers hydrogen bonding (H-bonding) with other compounds, making them to be promising candidates for photocatalysis. For example, Li et al. designed a supramolecular system composed of hydrazone-linked COF (BtE-COF) and Ni complex.[6] BtE-COF with abundant heteroatoms could generate intermolecular interaction with $Ni(bpy)_3^{2+}$ through the X···H-C (X = N, O, S) interactions, which achieved an excellent CO yield (2900 μmol $g^{-1}$). In addition, Zhang et al. prepared two hydrazone-linked COFs (i.e., AC-COF-1 with intralayer H-bonding and AC-COF-2 without H-bonding) and explored their photocatalytic performance.[11] Surprisingly, AC-COF-1 displayed remarkable metallaphotocatalysis performances owing to the decent visible-light harvesting capability as well as facile charge carrier transfer generated by H-bonding interactions. These results emphasized the importance of heteroatoms sites in photocatalytic reactions. In the photo-/electrocatalytic process, the abundant heteroatoms on the hydrazone bond can enhance the electronegativity of the material and endow it with some novel catalytic activity. Heteroatomic sites can also serve as redox active sites to improve the performance of hydrazone-linked COFs. For instance, Ma et al. prepared a hydrazone-linked redox-active COF (Redox-COF1) for the removal of $UO_2^{2+}$.[12] The results showed that Redox-COF1 performed well (ca. 97% at pH = 3) with a redox adsorption mechanism, which could effectively suppress the protonation of functional groups and efficiently facilitate the adsorption selectivity of $UO_2^{2+}$.

#### 2.1.3. Post-modification ability

With rich coordination sites, good chemical stability and diverse function groups, hydrazone-linked COFs can be further post-modified to produce desired materials. There are three possible post-modification strategies for hydrazone-linked COFs. Initially, hydrazone-linked COFs contain abundant N and O sites that can greatly expand their applications through interlayer interaction as well as coordination with different metal ions. In addition, hydrazone-linked COFs possess high structural stability that allows them to transform into more stable compounds by oxidation or cyclization. Moreover, hydrazone-linked COFs have many functional groups in the side chain that can be modified. Based on the above-mentioned three strategies, the post-modified hydrazone-linked COFs might have the following advantages like expanded functional diversity or enhanced structural stability. In the following section, we will give some examples to discuss the reported works about the post-modification of hydrazone-linked COFs.

At present, researchers have successfully introduced a large number of organic-inorganic functional components into hydrazone-linked COFs to obtain the required functional materials. For example, Zhang et al. synthesized a hydrazone-linked COF (Mo-COF) with the doping of molybdenum (Mo) through a bottom-up strategy for catalyzing selective oxidation.[13] With Mo sites aligning into the pore walls, Mo-COF performed better (＞99% conversion and 71% selectivity) than that of original COF (32% conversion and 7% selectivity). In addition, hydrazone-linked can be converted into a stable structure via oxidation or cyclization. For example, a hydrazide-linked MTH-TFPB COF was prepared by mild oxidation of a hydrazone-linked MTH-TFPB COF.[14] Interestingly, owing to the advantageous interaction between hydrazide moieties and $I_2$ molecules, hydrazide-MTH-TFPB COF showed higher $I_2$ uptake (3.05 g $g^{-1}$), which was ~1.3 times than hydrazone-MTH-TFPB COF. Another hydrazone-linked H-COF was converted into an oxadiazole-linked ODA-COF via post-oxidative cyclization.[15] Surprisingly, ODA-COF performed a higher hydrogen evolution rate (2615 μmol $g^{-1}$ $h^{-1}$) than that of the original H-COF (609 μmol $g^{-1}$ $h^{-1}$) because of the improved chemical stability and π-electron delocalization. Moreover, Li et al. reported a hydrazone-linked COF (SD-COF-3) with allyl group that could allow the post-modification through thiol-ene click reaction.[7a] Based on this, the authors introduced thioether sulfonate side chain into the skeleton and exfoliated it into LiCON-3 by lithiation. Because of its excellent stability and flexible anion side chains for $Li^+$ transport, LiCON-3 demonstrated a high ion conductivity ($10^{-5}$ S $cm^{-1}$) and a high $Li^+$ transference number (0.92) when utilized as solid electrolytes (SEs).

***Table 2.*** A summary of hydrazone-linked COFs with post-modification treatments.

| | COFs | Post-modification agents | Mehthods | Post-modification COFs | Ref. |
|---|---|---|---|---|---|
| 1 | COF | $MoO_2(acac)_2$ | Solvothermal | Mo-COF | [13] |
| 2 | COF-ASB (1) | $RuCl_3$ | Solvothermal | Ru@COF-ASB (2) | [21] |
| 3 | COF-AO (1) | $Pd(OAc)_2$ | Solvothermal | Pd@COF-AO (2) | [55] |
| 4 | Tf-DHzOPr-COF | Ru@CNT | Solvothermal | COF-Ru@CNT | [76] |
| 5 | SD-COF-1 | $C_3H_6O_2S$ | Light-assisted | SD-COF-2<br>SD-COF-3 | [38] |
| 6 | COF-42 | $H_2PdCl_4$ | Hydrothermal | COF@$Pd^{2+}$ | [53] |
| 7 | BTA-COF | $CuCl_2$ | Solvothermal | Cu-BTA-COF | [67] |
| 8 | Hydrazone-MTH-TFPB COF | $NaClO_2$ | Solvothermal | Hydrazide-MTH-TFPB COF | [14] |
| 9 | H-COF | $Cu(CF_3SO_3)_2$ | Solvothermal | ODA-COF | [15] |
| 10 | NAH-COF | LR/DMAP | Solvothermal | TDA-COF | [50] |

#### 2.1.4. Hydrolytic stability

The hydrazone bond (C=N-N) is formed by the condensation of hydrazine or hydrazide with an aldehyde. Compared with the parent imine linkage, the stability of hydrazine linkage would be stronger in water because the lone pair electrons in adjacent N atoms can be delocalized into C=N bonds, which reduces its electrophilicity to result in a highly stable structure in potential applications even under strong acid or base conditions in water.[16] For example, in 2013, Dichtel's group produced few-layer polymers by exfoliating a hydrazone-linked COF (COF-43) with high hydrolytic stability that could facilitate exfoliation.[8a] As expected, COF-43 showed high stability in many solvents (e.g., tetrahydrofuran, chloroform, toluene, and methanol) by solid and solution-state IR experiments. Based on the high stability, COF-43 enabled its exfoliation in different solvents and COF-based nanosheets could be obtained. In addition, during the synthesis of dual-pore COF (COF-OEt), Liang et al. utilized the high hydrolytic stability of hydrazone linkage and the instability of boroxine linkage.[8b] Owing to their dramatic difference, it was possible to achieve selective disassembly of the COF-OEt and it was confirmed by IR spectrum that the boroxine rings were totally hydrolyzed while keeping the hydrazone units unaffected. Based on this result, a kind of dual-pore COF was successfully prepared through this strategy. In addition, hydrazone-linked COFs with hydrolytic stability endow them with high processability in water. Recently, Fang et al. synthesized a range of hydrazone-linked COF films (i.e., CoP-TOB, CoP-TFPA and CoP-TFB) for electrocatalysis.[34] Owing to the good hydrolytic stability, the obtained film displayed good mechanical stability and was able to large-scale fabrication (up to 3000 $cm^2$ area). In addition, Ajnsztajn et al. reported the syntheses of a series of highly porous and crystalline hydrazone-linked COFs (i.e., TFB-DETH-COF, TFB-DBTH-COF and TFB-DHTH-COF) aerogels under the conditions of 90 vol% acetic acid along with 10 vol% acetonitrile or 10 vol% water.[17] Surprisingly, the TFB-DBTH and TFB-DHTH aerogels showed excellent stability in 3 M HCl, concentrated HCl, and 1 M NaOH, which proves the superior hydrolytic stability of hydrazone-linked COFs.

Moreover, the excellent stability of hydrazone-linked COFs is also beneficial for the separation in water under acid and base conditions. For example, Tang et al. have prepared two hydrazone-linked COF (TpDMTH) membranes for dye separation.[18] Expectedly, the TpDMTH-2 COF membrane showed no significant change in the performance or rejection of CR after immersing in HCl, NaOH and organic solvents (dioxane, acetone, methanol and ethanol) for 5 days, indicating its excellent stability. When compared with other imine-linked membranes (MPD-TFB/Nylon and TpPa/PVDF), the TpDMTH-2 COF membrane demonstrated higher permeance and rejection, which reveals the superiority of hydrazone-linked COFs to imine-linked COFs.

### 2.2. The preparation methods of hydrazone-linked COFs

Based on the above characteristics, hydrazone-linked COFs have been broadly researched and used in a variety of fields. In recent decades, hydrazone-linked COFs have been synthesized using various methods. In this part, the merits and disadvantages of many typical hydrazone-linked COF preparation methods (e.g., solvothermal, heating reflux, stirring, ball milling and interfacial synthesis) are discussed (Figure 5).

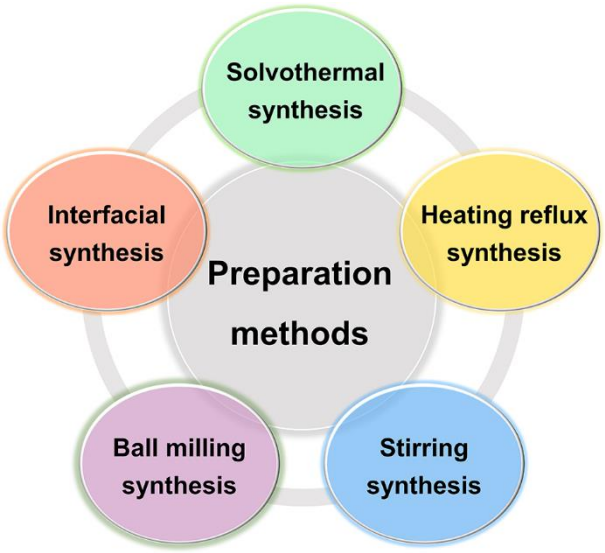


***Figure 5.*** Different preparation methods of hydrazone-linked COFs.

#### 2.2.1. Solvothermal synthesis

Solvothermal synthesis is the most typical synthesis method for hydrazone-linked COFs, which can be basically classified as Pyrex tube and reactor synthesis. Commonly, the steps for Pyrex tube synthesis method can be basically summarized: the Pyrex tube is firstly charged with ligands and solvents, frozen with liquid nitrogen, then freeze-vacuum-thaw for several times to remove oxygen from the tube; afterward, the Pyrex tube is then sealed *via* flame and heated for a certain time; finally, the obtained hydrazone-linked COFs are treated with multi-step purification steps to yield final products. The vast majority of hydrazone-linked COFs are synthesized based on this way owing to their commonly achieved good crystallinity. In 2011, Yaghi's group used this method to synthesize the first case of hydrazone-linked COF (COF-42) with the reaction of 2,5-diethoxyterephthalohydrazide (DETH) and 1,3,5-triformylbenzene (TFB) under the conditions of mesitylene and dioxane (Figure 6a).[3i] Its good crystallinity was confirmed by powder X-ray diffraction (PXRD) and Ar adsorption isotherm (Figure 6 b-c). However, this method still has the disadvantages like relatively complicated vacuum and flame treatment procedures, and generally needed one to several days to complete the reaction.

10.1002/anie.202404941



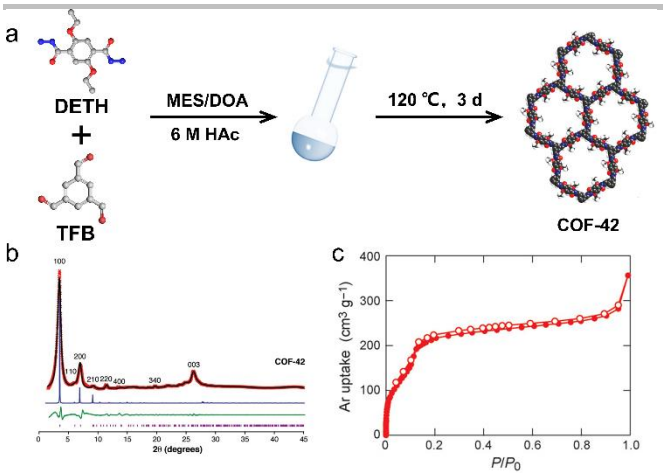


***Figure 6.*** Synthesis and characterization of COF-42. a) Schematic representation of solvothermal synthesis using Pyrex tube. b) PXRD pattern. c) Ar adsorption and desorption isotherm. Reproduced with permission.[3i] Copyright 2011, American Chemical Society.

Reactor synthesis is another solvothermal strategy for the batch preparation of hydrazone-linked COFs. However, up to date, only a limited number of hydrazone-linked COFs have been prepared based on reactor synthesis. For example, COF BTT-DGMH was prepared by dispersing benzotrithiophene tricarbaldehyde (BTT) and 1,3-diaminoguanidine hydrochloride (DGMH) in a mixed solution of mesitylene, dioxane and 6M aqueous acetic acid (AcOH) (Figure 7a).[19] After that, the above-mixed solution was transferred into a polytetrafluoroethylene reactor liner. At last, the liner was put into a reactor shell, heated at 120 °C and rested for 3 days. After filtration and washing by methanol and tetrahydrofuran, the sample was dried in a vacuum freeze dryer and 72% yield was achieved. In addition, PXRD tests were performed to demonstrate its crystal structure and $N_2$ adsorption/desorption isotherms were conducted to illustrate its permanent porosity (Figure 7b-c).

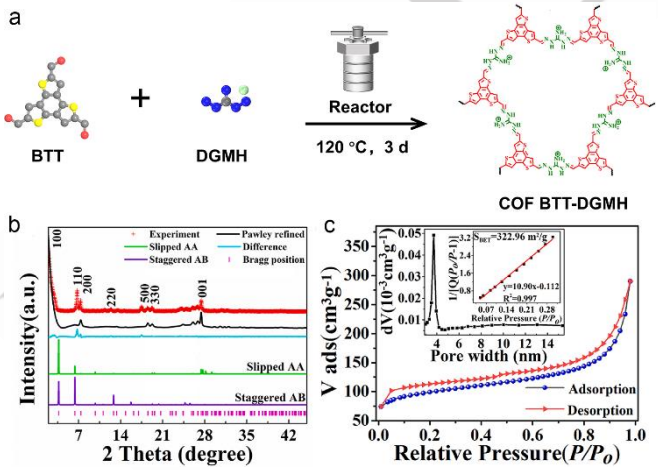


***Figure 7.*** Synthesis and characterization of COF BTT-DGMH. a) Schematic diagram of solvothermal synthesis using reactor. b) PXRD pattern. c) $N_2$ adsorption curve. Reproduced with permission.[19] Copyright 2022, Elsevier.

### 2.2.2. Solvothermal synthesis

Heating reflux is another method used to synthesize hydrazone-linked COFs. Compared with the solvothermal method, this method is relatively simpler to operate without complicated procedure of pipeline sealing. Taking Tp-$DG_{Cl}$ as an example (Figure 8a), 1,3-diaminoguanidine hydrochloride ($DG_{Cl}$) and 1,3,5-triformylbenzene (Tp) were dissolved into the deionized water (DI) and 1,4-dioxane, refluxed and stirred for 24 h at 120 °C to successfully produce Tp-$DG_{Cl}$.[20] Besides, the PXRD pattern and Fourier transform infrared (FT-IR) spectra have been carried out to confirm its structure and component (Figure 8b-c).

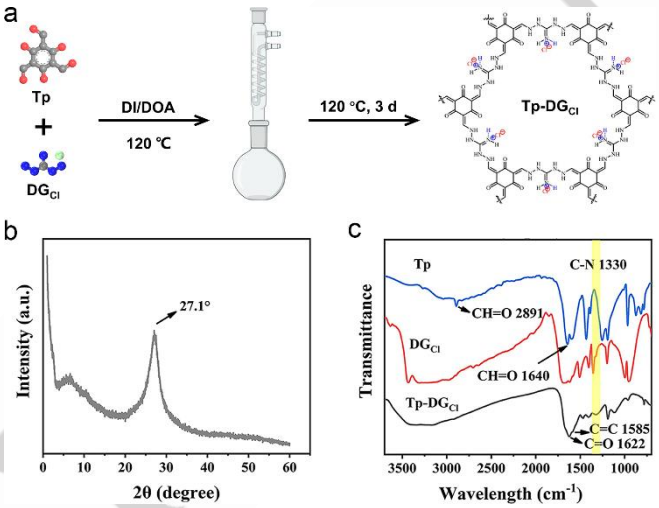


***Figure 8.*** Synthesis and characterization of Tp-$DG_{Cl}$. a) Schematic diagram of heating reflux synthesis. b) PXRD pattern. c) FT-IR spectra. Reproduced with permission.[20] Copyright 2021 Elsevier.

### 2.2.3. Stirring synthesis

Stirring method is a kind of facile method to yield hydrazone-linked COFs. It is usually conducted by adding the monomers to the targeted solution and stirring it with or without heating procedures. Although it has the advantages like simple and easy operation process, it is still limited to a small number of simple ligands. In 2018, the stirring method could be applied to generate COF-ASB (1) by the simple stirring procedures at 120 °C for 72 h based on the reaction of benzene-1,4-dicarboxaldehyde (BDA), benzene-1,3,5-tricarbohydrazide (Bth) and AcOH in N, N-dimethylformamide (DMF) (Figure 9a).[21] The microcrystalline COF-ASB (1) with a well-defined structure was demonstrated in Figure 9b. The transmission electron microscope (TEM) image of COF-ASB (1) displayed the well-order stacking of layers, proving its good crystallinity (Figure 9c).

10.1002/anie.202404941



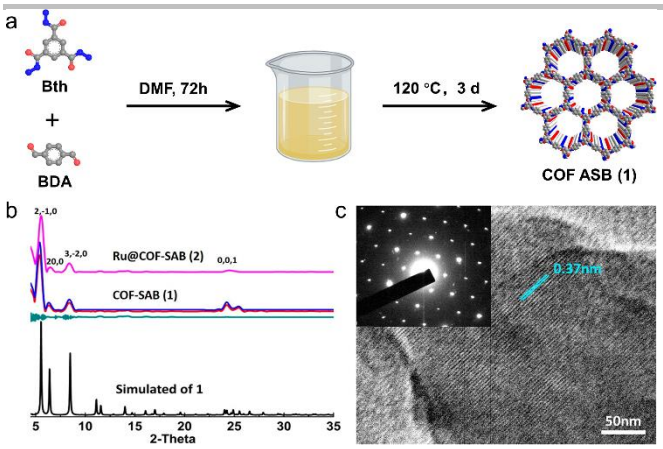


***Figure 9.*** Synthesis and characterization of COF ASB (1). a) Schematic diagram of stirring synthesis. b) PXRD pattern. c) HRTEM image and the electron of COF ASB (1). Reproduced with permission.[21] Copyright 2018, American Chemical Society.

### 2.2.4. Ball milling synthesis

Compared to the stirring synthesis, ball milling synthesis is another facile method to produce hydrazone-linked COFs. When compared to conventional synthesis, ball milling synthesis has gained great attention owing to its fast and eco-friendly procedure. For example, in 2014, Banerjee's group prepared a novel hydrazone-linked COF TpTh using this method.[22] During the synthesis, Tp and Terephthalic dihydrazide (Th) were added in the mixture of mesitylene, dioxane and 3 M AcOH in a ball milling jar and milled in a Retsch MM400 mill (25 Hz). After 90 min, the obtained sample was washed with N, N-dimethylacetamide (DMA), DMF and acetone. Although this method has attractive characteristics like short time and ease in operation, the accessible examples of hydrazone-linked COFs are still rare and need more efforts to expand the types of hydrazone-linked COFs.

### 2.2.5. Interfacial synthesis

Up to date, the reported works about interfacial synthesis include liquid-liquid (e.g., oil-water and oil-water-oil), liquid-air and solid-gas modes. For example, Ma's group covered an example for oil-water mode to synthesize Redox-COF1 that is beneficial to the selective adsorption of $UO_2^{2+}$.[12] During the synthesis, 25 mg benzene-1,3,5-tricarbohydrazide (BTCH) was dissolved in 6M AcOH to give the amine solution (A); and aldehyde solution (B) was produced by dissolving 25 mg 2,5-dihydroxyterephthalaldehyde (DHPA) in dichloromethane ($CH_2Cl_2$). Then, the solution A was dropped slowly to the top of the solution B. After a certain time, the obtained sample was washed with $CH_2Cl_2$, ethanol, acetone and DMF. It could be applied to the adsorption of $UO_2^{2+}$ with a 97% selectivity. In addition, another example for oil-water-oil mode was applied for the synthesis of a kind of ionic hydrazone-linked COFs nanosheets ($DhaTG_{Cl}iCONs$).[23] Specifically, the middle water phase cooperated with the two oil phases could serve as the function of confined reaction region and reservoirs for storing/supplying ligands, respectively. In detail, DHPA was first dissolved in $CH_2Cl_2$ and placed in a glass beaker as the bottom oil phase. Then, 3 M AcOH was added to the surface of the aldehyde solution. Subsequently, $TG_{Cl}$ dissolved in DMF was slowly added onto the AcOH phase as the top phase. After 7 days, $DhaTG_{Cl}iCONs$ with a few-layer thickness (1.2 ± 0.08 nm), large lateral size (at least 20 μm), and high crystallinity was achieved.[23]

Except for liquid-liquid mode, liquid-air mode has been used for interfacial synthesis of hydrazone-linked COFs. An example for liquid-air mode is the fabricating metalloporphyrin-based hydrazone-linked COF films.[8c] Take the synthesis of CoP-TOB as an example, 2,4,6-tris(4-formylphenoxy)-1,3,5-triazine (TOB) and Co porphyrin (CoP) were initially dissolved in dimethyl sulfoxide (DMSO). Then, CoP with amphiphilicity tended to gather at the liquid-air interface and reacted with TOB to produce the film product (CoP-TOB) (Figure 10a). As shown in Figure 10b, CoP-TOB could achieve large-scale preparation (up to 3000 $cm^2$). Additionally, it could be bent during the pressing test (Figure 10c). The obtained CoP-TOB film could tolerate and hang a weight of 20 g and 30 g, indicating its relatively high mechanical properties (Figure 10d-e). Although interfacial synthesis requires a large number of organic solvents and relatively complex steps, this synthesis method is still suitable for preparing hydrazone-linked COFs with nanoscale forms (e.g., nanosheets and films).

In addition, chemical vapor deposition (CVD) as a kind of solid-gas processing strategy has also been applied for interfacial synthesis. For example, Duam et al. reported a defect-free hydrazone-linked COFs films utilizing CVD approach.[24] During the synthesis, the two monomers (TFB and DETH) were placed on $SiO_2$/Si substrate in a tube furnace. After that, the tube furnace was evacuated to 3 Torr pressure and heated under argon gas atmosphere. After 30 min, a kind of large area COF-42 film was produced, which holds much promise in the generation of scalable COF films in a short time.

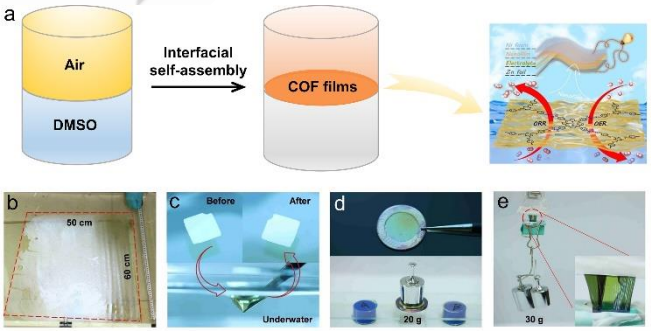


***Figure 10.*** Synthesis and performances of COP-TOB film. a) Schematic diagram of interfacial synthesis. b) Photograph. c) Pressing test. d) Weight-supporting test. e) Hanging test. Reproduced with permission.[8c] Copyright 2022, Wiley-VCH.

## 3. Applications of hydrazone-linked COFs

Based on the above-mentioned advantages (e.g., structural flexibility, heteroatomic sites, post-modification ability and hydrolytic stability) and various preparation methods, hydrazone-linked COFs show much potential in various aspects. To date, a broad range of applications (e.g., adsorption/separation, catalysis, chemical sensing, energy storage) have been developed for hydrazone-linked COFs (Figure 11). The following section will discuss the reported works of hydrazone-linked COFs in these applications.

10.1002/anie.202404941





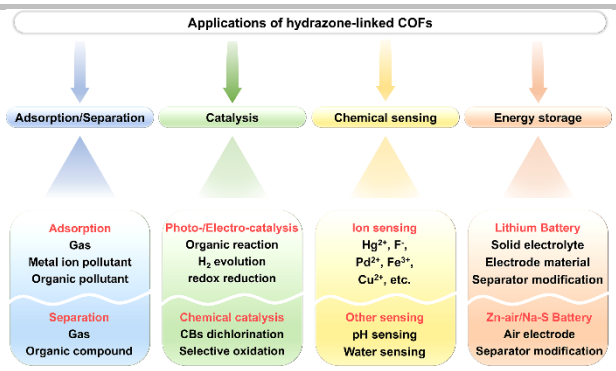


***Figure 11.*** The main applications of hydrazone-linked COFs.

### 3.1. Adsorption

Owing to the abundant N/O atom sites, structural flexibility and high hydrolytic stability compared to other Schiff-based COFs, hydrazone-linked COFs are promising candidates for adsorption and separation. At present, the reported adsorption applications of hydrazone-linked COFs can be mainly classified as the adsorption of metal ion pollutant, organic pollutant and gas. Meanwhile, the separation of hydrazone-linked COFs mainly includes the separation of gas and organic compound. The following sections will discuss this content in detail.

#### 3.1.1. Adsorption of metal ion pollutant

Metal ions are widely used in the production of chemicals and it is essential to recover heavy metal ions from water due to their toxicity, persistence and availability.[25] Adsorption is the most commonly used recovery method with low cost and wide application range.[26] Being among the newest categories of porous materials, hydrazone-linked COFs with properties of crystalline skeleton, porous structure, high stability, and tunable functions can be regarded as potential adsorbing materials for metal ion pollutant.

Recently, a guanidinium-based hydrazone-linked COF (BT-$DG_{Cl}$) showed remarkable performance for the elimination of hazardous $Cr^{6+}$.[27] Owing to the robust binding forces between diamino-guanidinium units and tetrahedral oxyanions, and the ion exchange mechanism, BT-$DG_{Cl}$ functioned primarily and was able to quickly decrease the $Cr^{6+}$ concentration (1 ppm to 10 ppb). Along the same line, a guanidinium-based hydrazone-linked COF (Tp-$DG_{Cl}$) was likewise prepared for removing $Cr^{6+}$ (Figure 12a), achieving an excellent adsorption and loading capacity (360.02 mg $g^{-1}$) through synergism of ion exchange and electrostatic attraction (Figure 12b-e).[20] Besides, another hydrazone-linked TpODH COF performed good adsorption capacities of $Cu^{2+}$ (324 mg $g^{-1}$) and $Hg^{2+}$ (1692 mg $g^{-1}$).[28] Such high capacity may be explained by the numerous N/O sites periodically aligned on the pore walls of TpODH and good interaction toward the metal ions. Furthermore, two kinds of chitosan membranes integrated with TpODH were proposed considering the limitations of COF powders.[29] It not only possessed hierarchically porous structure and high specific surface area, but also demonstrated unprecedented adsorption capacities for $Cu^{2+}$ (144 mg $g^{-1}$) and $Cr^{6+}$ (388 mg $g^{-1}$), which illustrated its potential on adsorption of metal ions.

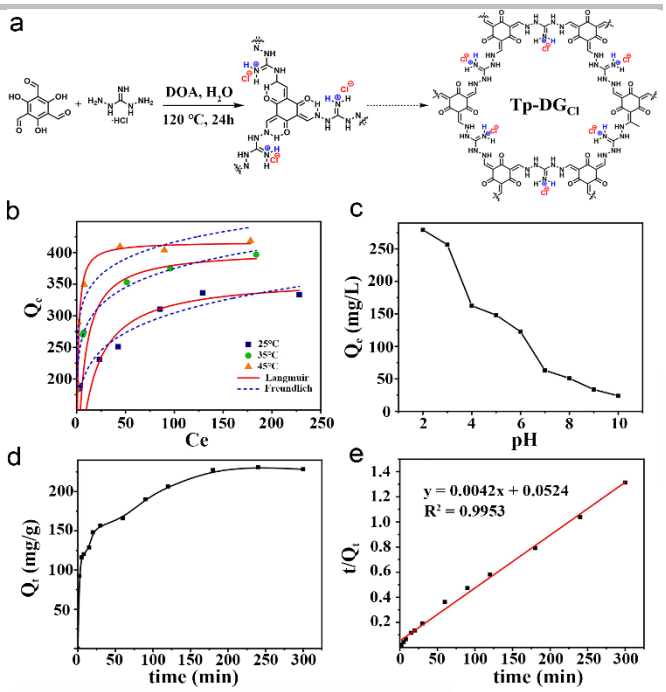


***Figure 12.*** Tp-$DG_{Cl}$ and its $Cr^{6+}$ adsorption performance. a) Synthesis route. b) Temperature-dependent adsorption isotherm. c) The pH impacts on the performance. d) Adsorption kinetics of $Cr^{6+}$. e) Linear fitting. Reproduced with permission.[20] Copyright 2021, Elsevier.

Aside from some traditional metal ions, hydrazone-linked COFs can also remove certain radioactive ions. For instance, a hydrazone-linked iCON ($DhaTG_{Cl}$) was put forward for the removal of $ReO_4^-$.[30] Combined with hydroxyl groups and $Cl^-$ that were weakly linked within the channels of cationic knots, $DhaTG_{Cl}$ demonstrated a 437 mg $g^{-1}$ adsorption capacity with a 5.0 × $10^5$ distribution coefficient toward $ReO_4^-$. Moreover, Li et al. reported a case of 2D CONs (Redox-COF1) for the adsorption of $UO_2^{2+}$ (Figure 13a).[12] Interestingly, owing to the redox adsorption mechanism, Redox-COF1 could achieve extraordinary adsorption (97% selectivity at pH = 3) for $UO_2^{2+}$ (Figure 13b). Additionally, three hydrazone-linked COFs (i.e., COF-JLU4, COF-IHEP10 and COF-IHPE11) with different phosphonate units on their side chains were developed.[31] Notably, COF-IHPE11 with phosphonate contents in the skeleton achieved a high adsorption capacity for $UO_2^{2+}$ (~110 mg $g^{-1}$) while the uptake of COF-JLU4 is less than 70 mg $g^{-1}$. Theoretical calculations suggested that the exceptional performance of COF-IHEP11 was attributed to the combined influence of phosphonate concentrations and carbonyl groups.

10.1002/anie.202404941





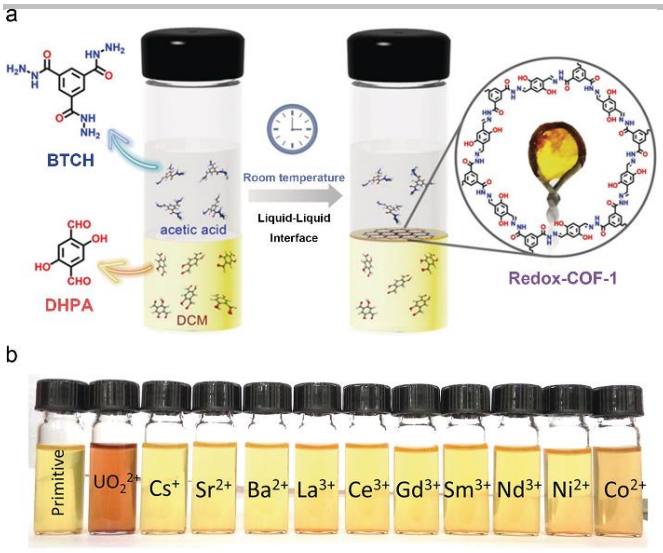


***Figure 13.*** Redox-COF1 and its metal ion adsorption performance. a) Synthetic route. b) The photo images of the suspensions after adding various metal ions. Reproduced with permission.[12] Copyright 2019, Wiley-VCH.

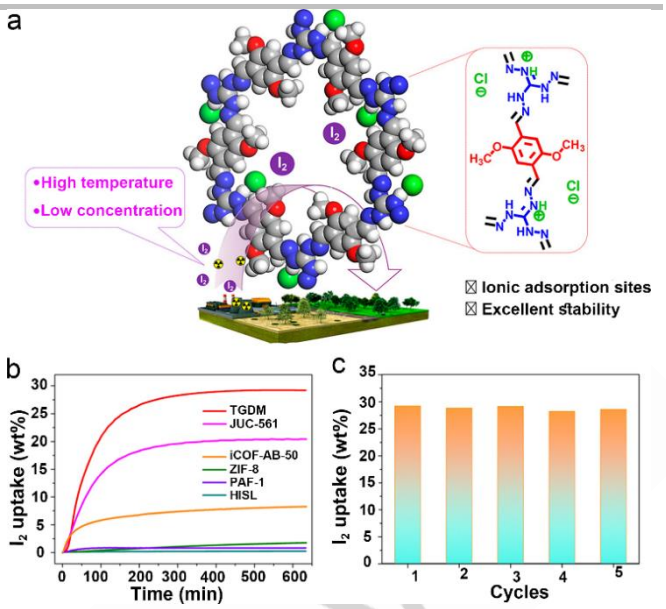


***Figure 14.*** $I_2$ adsorption diagram and performance of TGDM. a) Ionic adsorption sites on TGDM. b) $I_2$ adsorption performances of various adsorbing materials. c) Recyclability tests. Reproduced with permission.[35] Copyright 2022, American Chemical Society.

### 3.1.2. Adsorption of organic pollutant

In addition to removing the heavy metal ion from metal ion pollutants, hydrazone-linked COFs can also be used to adsorb organic pollutants such as 2,4-dichlorophenol, $I_2$ and so on. For example, three hydrazone-linked iCOFs (i.e., TFPA-$TG_{Cl}$-iCOF, TFPT-$TG_{Cl}$-iCOF and TFPB-$TG_{Cl}$-iCOF) were reported for removing 2,4-dichlorophenol.[32] Interestingly, TFPT-$TG_{Cl}$-iCOF with high crystallinity, cationic sites and hydrogen bonding sites displayed a good 893 mg $g^{-1}$ adsorption capacity. Except for the removal of 2,4-dichlorophenol, it is essential to develop novel and effective approaches for $I_2$ capture owing to the rapid growth of radioactive $I_2$ caused by nuclear energy technique.[33] In general, adsorption materials with electron-rich units might form electron transfer complexes with the electron-deficient iodine elements.[34] Given this, a hydrazide-MTH-TFPB COF was prepared by mildly oxidizing a hydrazone-MTH-TFPB COF for removing $I_2$.[14] Benefiting from its extended network skeleton and plentiful hydrazide units, hydrazide-MTH-TFPB COF exhibited excellent adsorption of $I_2$ vapor (3.05 g $g^{-1}$) than its precursor. In addition, Zhang et al. developed a hydrazone-linked COF (TGDM) and achieved excellent high-temperature $I_2$ capture performance with abundant ionic guanidinium groups (Figure 14a).[35] Figure 14b revealed that in the first 120 min, TGDM could rapidly adsorb $I_2$ (~23 wt%) and ultimately reach up to 29.24 wt% after extending time. Moreover, TGDM could maintain over 97% of its initial $I_2$ adsorption capacity after five cycles (Figure 14c). Furthermore, Cai's group proposed an amine-functionalized COF ($NH_2$-Th-Bta COF) to be applied in $I_2$ capture.[36] Interestingly, $NH_2$-Th-Bta COF displayed a 3.58 g $g^{-1}$ $I_2$ uptake capacity, which is much higher than its nonfunctionalized one (0.68 g $g^{-1}$). Furthermore, it showed remarkable recycling ability with maintained high $I_2$ adsorption after six cycles. Although many articles have reported inspired works about hydrazone-linked COFs that could be employed in efficient $I_2$ adsorption, their further use of absorbed $I_2$ for otherwise applications like catalysis is more designable.

### 3.1.3. Gas adsorption

In addition to metal ion pollutant and organic pollutant, gas adsorption has also received widespread attention. Currently, gas adsorption is mainly focused on $CO_2$, and there are few reports on other gases. Hydrazone-linked COFs can be applied in $CO_2$ capture stemmed from their abundant N atoms and porous structure. For instance, a stable TPT/OH COF was synthesized and employed for efficient $CO_2$ capture.[37] Owing to the N-rich skeleton that could interact with $CO_2$ (Lewis acidic molecules), TPT/OH COF demonstrated a high $CO_2$ adsorption ability (0.9 mmol $g^{-1}$) at 25 ℃ (1 bar). In addition, Sun et al. synthesized three N-rich hydrazone-linked COFs (i.e., COF-SDU1, COF-SDU2 and COF-SDU3) to explore relative influence factor for $CO_2$ adsorption.[38] The results showed that $CO_2$ capacity could be largely enhanced with large pore size (COF-SDU1~741 mg $g^{-1}$, COF-SDU2~484 mg $g^{-1}$, COF-SDU3~331 mg $g^{-1}$.) at a relatively high pressure (>25 bar). Except for the influence of pore size, function groups also play a vital role in enhancing $CO_2$ adsorption. For instance, coCOF-H and coCOF-OH were modified with a tertiary amine group to achieve amine-coCOF-H and amine-coCOF-OH with a mixed linker method.[39] It was shown the functionalized linker species could exhibited a better interaction with $CO_2$, which was revealed by an improved relative $CO_2$ adsorption ability (2.22 μmol $m^{-2}$ for amine-coCOF-H and 2.52 μmol $m^{-2}$ for amine-coCOF-OH). These results illustrated that the tuning of pore sizes and function groups would affect the performance of $CO_2$ adsorption, and we hope more advanced strategies can be explored to enrich the diversity of $CO_2$ adsorption materials based on hydrazone-linked COFs.

### 3.2. Separation

In addition to the above adsorption applications, hydrazone-linked COFs can also be used in separation applications for a series of mixtures such as biogas, toluene/n-heptane mixture,

10.1002/anie.202404941



Congo Red solution, aromatic/aliphatic mixture, and so on. For instance, Jiang et al. used an oil-water-oil triphase strategy to prepare $DhaTG_{Cl}$ iCOFNs (Figure 15a).[23] As illustrated in Figure 15b-c, the scanning electron microscopy (SEM) image and the TEM image reflected the uniform nanosheet morphology. In addition, the atomic force microscopy (AFM) image showed the nanosheet with a 1.2 ± 0.08 nm thickness (Figure 15d). The iCOFNs was further processed into a COF membrane for the separation of biogas. Notably, the membrane displayed high $CO_2$ permeance (316 GPU) and $CO_2/CH_4$ gas mixture selectivity (49), and good stability under 5 bar pressure.

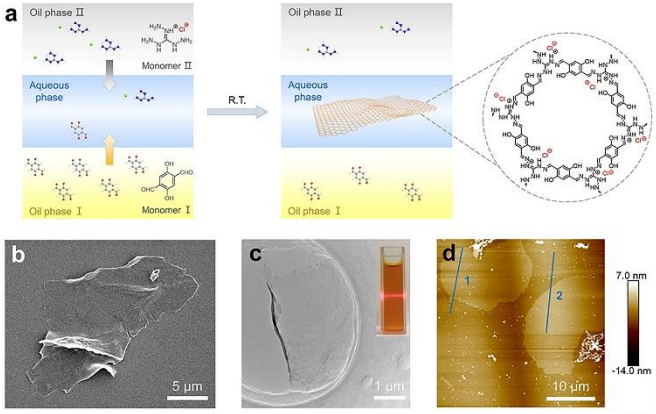


***Figure 15.*** Synthesis and characterization of $DhaTG_{Cl}$ iCONs. a) Schematic diagram of triphase synthesis. b) SEM image. c) TEM image and Tyndall effect of suspension. d) AFM image. Reproduced with permission.[23] Copyright 2021, Wiley-VCH.

Except for the separation of biogas, separating toluene/n-heptane was also explored. For example, An's group modified $Ag^+$ in the structure of COF-LZU8 and hybridized it with poly (ether-blockamide) (Pebax 2533) to generate a membrane.[40] When compared to the original Pebax membrane, the optimized membrane demonstrated a 293 g $m^{-2}$ $h^{-1}$ permeation flux and 4.03 separation factor. Besides, Tang's group prepared a self-standing hydrazone-linked COF membrane (TpDMTH membrane) for the separation of Congo Red solution.[18] The optimized TpDMTH membrane demonstrated a performance of 109.73 L $m^{-2}$ $h^{-1}$ $bar^{-1}$ and a high rejection of 99.56% for Congo Red solution. The performance could be ascribed to the interaction caused by size sieving and the Donnan effect. Furthermore, hydrazone-linked COFs were also used as a coating material for columns and can be used in the isomer separation. For example, a novel hydrazone-linked chiral COF equipped with $SiO_2$ (BtaMth-COF@$SiO_2$) has been reported.[41] It demonstrated high resolution performances for separating positional isomers of nitrotoluene (1.08/1.10) and nitrochlorobenzene (1.13/1.06), and cis-transisomers of beta-cypermethrin (1.18) and metconazole (1.21). In another case, Chen's group prepared three COFs (i.e., COF-LZU8, COF-LZU1 and COF-42) with different hydrazone linkage and side-chains.[42] It has been shown that COF-LZU8 possessing hydrazone linkage and longer side chains performed better (oretical plate number = 6.39 × $10^4$ for diethyl phthalate, 5.30 × $10^4$ for diallyl phthalate, 4.96 × $10^4$ for diisopropyl phthalate and 3.48 × $10^4$ for dipropyl phthalate) when it comes to separating analytes with larger molecular sizes.

### 3.3. Catalysis

Hydrazone-linked COFs possess advantages of designable structure and heteroatomic atoms, which endow them with good catalytic performance. In general, the active sites of hydrazone-linked COFs come from the functional moieties on the structure skeleton by in-situ structure design or post-modification treatment. These results make hydrazone-linked COFs exhibit great potential for broadening applications in photocatalysis, electrocatalysis and chemical catalysis and so on. In this section, a detailed introduction to catalysis will be discussed.

#### 3.3.1. Photocatalysis

Photocatalysis is regarded as an eco-friendly solution for treating environmental and energy issues.[43] Specifically, hydrazone-linked COFs can be well-designed at the molecular level to serve as functional photocatalysts. To date, efforts have been dedicated to developing hydrazone-linked COF photocatalysts to investigate the structure-property correlation in photocatalytic applications.

Recently, some pioneering works on the application of photoactive hydrazone-linked COFs as heterogeneous photocatalysts in organic synthesis have been reported.[11,44] For instance, a hydrazone-linked COF (TFPT-ODH) has been reported with high photocatalytic performance in the photo-cyclization of 2-isocyanodiaryl compounds and phenylhydrazine, obtaining a 75-92% yield for phenanthridines.[44a] A photocatalytic mechanism was proposed: under light irradiation, pairs of electrons and holes could be generated by TFPT-ODH; then $O_2^{\bullet-}$ and $^1O_2$ were produced through the oxygen activation by photogenerated electrons. Meanwhile, TFPT-ODH* was converted into TFPT-ODH$^{\bullet+}$ to catalyze the photo-cyclization reaction. In addition, the reaction of addition cyclization was also investigated. Yang's group prepared a hydrazone-linked 2D-COF-1 to catalyze 2-arylphenyl isocyanides to generate varied 6-substituted-phenanthridines.[44b] Notably, it could achieve a 77% yield when using 2D-COF-1 as heterogeneous photosensitizer. Besides, a hydrazone-linked TFB-COF was synthesized and applied in cross-dehydrogenative coupling (CDC) reactions.[44c] TFB-COF, possessing high porosity and efficient light-harvesting ability, could achieve an 87% yield for catalyzing the CDC reaction of N-aryltetrahydroisoquinoline.

Furthermore, a hydrophilic hydrazone-linked TFPT-BMTH-COF was reported and applied in the transformation of benzylamines to imines.[44f] Benefiting from the hydrophilic group periodically arranging on the channels and strong interlayer interaction in the structure, it displayed exceptional photocatalytic activity (conversion rate, 99%) in water and environmentally benign properties. In another case, a range of pillararene-based hydrazone-linked COFs (NP5-based COFs) with diverse active sites were presented and employed for catalyzing the coupling reactions of benzylamine (Figure 16).[44e] Surprisingly, all samples displayed high performance (conversion rate, 99% and selectivity, >98%) because of the improved light absorption ability and charge transfer efficiency induced by the well-ordered and electron-rich structure. In another example, a hydrazone-linked COF (2D-COF-1) was prepared and used for catalyzing C3 arylation and alkylation of quinoxalin-2(1H)-ones.[44d] Remarkably, it could achieve an 83% yield for desired alkylation product owing to its high chemical stability and heterogeneous nature. Besides,

10.1002/anie.202404941



another hydrazone-linked COF (TFB-BMTH) was designed and displayed exceptional photocatalytic activity (yield, 99%) in the hydroxylation reaction for arylboronic acid as well as excellent cycling ability.[44g] More recently, Zhang's group designed and synthesized an acetylene-based hydrazone-linked AC-COF-1 for the metallaphotocatalytic amination of aryl chlorides.[11] Remarkably, AC-COF-1/Ni system achieved a 99% yield of C-N coupling products from various aryl chloride substrates. These works have proved the exceptional photocatalytic ability of hydrazone-linked COFs, which hold much potential in organic synthesis.

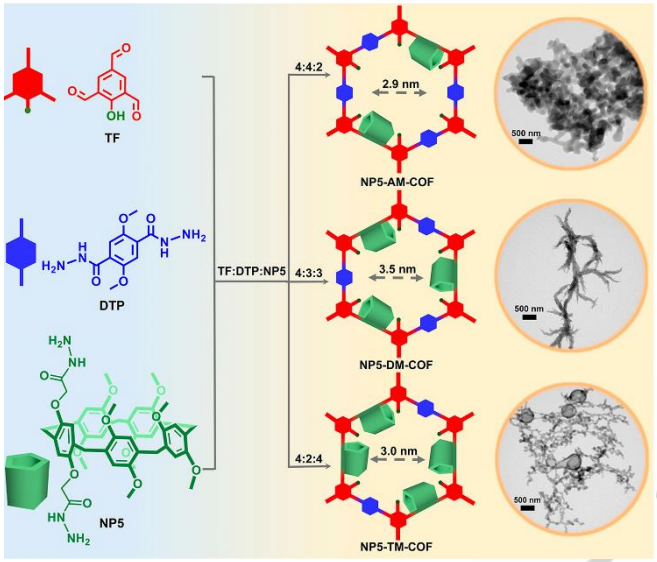


***Figure 16.*** Diagrammatic representation of the NP5-based COFs with different building blocks. Reproduced with permission.[44e] Copyright, 2022, American Chemical Society.

Photocatalytic hydrogen production has garnered significant interest as hydrogen is regarded as the most promising sustainable energy source.[45] So far, there are some reports on hydrogen evolution using hydrazone-linked COFs. For example, Lotsch et al. designed a hydrazone-linked COF (TFPT-COF) that could be applied in hydrogen evolution in 2014.[46] TFPT-COF is represented as a lightweight and efficient (1970 μmol $h^{-1}g^{-1}$ under standard basic conditions) model system, which might serve as promising catalyzers for practical applications of hydrogen evolution. Furthermore, Lotsch et al. developed two hybrid cocatalysts (i.e., [**Co-1a**]-COF and [**Co-1b**]-COF).[47] They showed high photocatalytic activity (photonic efficiency, [**Co-1a**]-COF, 0.14% and [**Co-1b**]-COF, 0.11%). The improvement of the reaction activity and hindering degradation of the catalyst was ascribed to the genuine interaction between the COF backbone and the cobaloxime.

In addition to being used as a catalyst, hydrazone-linked COF could also serve as a modifier on the surface of MOFs, thereby exerting a synergistic effect between them. For example, Jiang and co-workers grew a TFPT-DETH COF on the $NH_2$-UiO-66 surface to generate a MOF@COF material ($NH_2$-UiO-66@TFPT-DETH) with suitable shell thickness (~20 nm).[48] Owing to the synergistic effect within the core-shell framework, the optimal material achieved a higher hydrogen evolution rate (7178 μmol $g^{-1}$ $h^{-1}$) than that of origin TFPT-DETH (2301 μmol $g^{-1}$ $h^{-1}$) and physically mixed counterpart (992.3 μmol $g^{-1}$ $h^{-1}$). Hydrazone-linked COFs could also be further transformed into a more stable and functional form for performance exploration. In 2022, an oxadiazole-linked ODA-COF with π-conjugated units was achieved from a hydrazone-linked H-COF through post-oxidative cyclization.[15] Upon visible light irradiation, it achieved a higher hydrogen evolution rate (2615 μmol $g^{-1}$ $h^{-1}$) than that of pristine H-COF (609 μmol $g^{-1}$ $h^{-1}$). Recently, another four hydrazone-linked COFs (i.e., BTT-Hz-1, BTT-Hz-2, TFB-Hz-1 and TFB-Hz-1) were produced (Figure 17a).[49] Interestingly, BTT-Hz-1 and BTT-Hz-2 with electron-rich and conjugated units showed a higher photocatalytic $H_2$ evolution rate of 17.27 mmol $g^{-1}$ $h^{-1}$ and 3.89 mmol $g^{-1}$ $h^{-1}$ than TFB-Hz-1 and TFB-Hz-1 (no $H_2$ detected for TFB-Hz-1 and TFB-Hz-1) (Figure 17b-c).

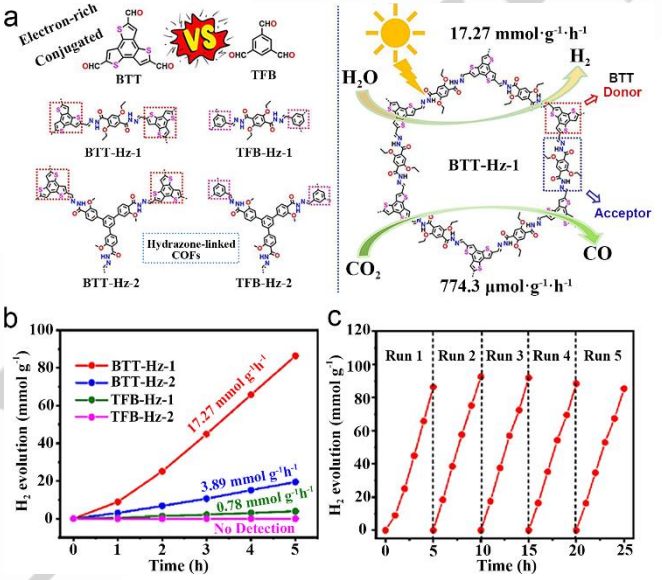


***Figure 17.*** Schematic representation and photocatalytic hydrogen evolution performances of the four hydrazone-linked COFs. a) Schematic illustration of BTT-Hz-1, BTT-Hz-2, TFB-Hz-1 and TFB-Hz-2. b) The performances of BTT-Hz-1, BTT-Hz-2, TFB-Hz-1 and TFB-Hz-2. c) Recycling tests of BTT-Hz-1. Reproduced with permission.[49] Copyright 2023, Elsevier.

Carbon capture and storage is a crucial tactic for reducing the greenhouse effect. In 2020, Su's group have synthesized a hydrazone-linked COF (NAHN-Tp) and combined it with [Ir-ppy] to achieve excellent visible-light absorption for photocatalytic $CO_2$ reduction.[50] For a 1 h reaction, it performed a higher CO evolution rate (88.6 μmol) with a selectivity of 98% than that of [Ir-ppy]. Meaningfully, the COF/[Ir-ppy] catalyst could be stable for 7 h, which showed better performance than [Ir-ppy] (30 min). Recently, Li et al. reported a COF-based photosystem ($Ni(bpy)_3$@BtE-COF) for photocatalytic $CO_2$ reduction.[6] The hydrogen-bond interactions that existed in COF and $Ni(bpy)_3$ both mediated the charge transfer and inhibited the back electron transfer. Interestingly, it performed good CO generation (2900 μmol$g^{-1}$ with 88% selectivity) over $H_2$ production after a 4 h reaction.

In addition to hydrogen evolution and $CO_2$ reduction, hydrazone-linked COFs are also used for other purposes in photocatalysis. For instance, Li's group synthesized a hydrazone-linked COF (DETH-COF) that achieved an excellent $H_2O_2$ yield rate of 1.0 mmol $g^{-1}$ $h^{-1}$ in pure water under atmospheric circumstances.[51] It was demonstrated that the hydration of the

10.1002/anie.202404941



hydrazone linkage in COFs initiated the water oxidation. In addition, Ma et al. constructed a series of isoreticular hydrazone-linked COF photocatalysts with excellent optical and electronic properties.[52] For example, COF-4 showed a better photocatalytic uranium extraction performance (~6.84 $mg^{-1}$ $g^{-1}$) in seawater, which could be ascribed to superior excited electron utilization efficiency and charge transfer ability. Moreover, Jiang et al. constructed four COFs with different linkages.[53] Surprisingly, for their applications of photocatalytic activity in $H_2O_2$ production, the hydrazone-linked Hz-TFPPy-DETHz-COF can produce $H_2O_2$ with an excellent rate of 1,555 μmol $g^{-1}$ $h^{-1}$, which is almost twice higher than imine-linked Im-TFPPy-PDA-COF (812 μmol $g^{-1}$ $h^{-1}$). The better performance of hydrazone-linked Hz-TFPPy-DETHz-COF might be attributed to the non-conjugated structure that enables a better utilization of LUMO level energy to promote the electron transfer for oxygen reduction and thus the $H_2O_2$ production.

### 3.3.2. Electrocatalysis

Electrocatalysis technology provides a variety of methods for energy storage and conversion and is a significant way to achieve green and clean energy in the future. In 2020, Chen et al. constructed a COF@Pd@PEDOT hybrid material *via* polymerizing EDOT monomer with $PdCl_4^{2-}$ as an oxidant, showing enhanced catalytic performance for ethanol electro-oxidation.[54]. The optimal material exhibited a higher mass activity (607 mA $mg^{-1}$) than that of the commercial catalyst of Pd/C (359 mA $mg^{-1}$). Moreover, it displayed exceptional recycling ability. Additionally, Tang et al. reported the fabrication of a series of hydrazone-linked COF films (i.e., CoP-TOB, CoP-TFPA and CoP-TFB) based on metalloporphyrin component for electrocatalysis.[8c] These films exhibited excellent mechanical stability and structural integrity and could be scaled up to 3000 $cm^2$ area. Their electrocatalytic oxygen reduction reaction (ORR) activity was confirmed by cyclic voltammetry test. Additionally, their oxygen evolution reaction (OER) activity was further verified by overpotential and tafel slope tests. These three catalysts exhibited catalytic activity for both ORR and OER simultaneously, which showed much potential in redox electrocatalysis.

### 3.3.3. Chemical catalysis

Chemical catalysis plays an important role in modern industrial production processes due to its efficient and economical characteristics.[55] In addition to the photocatalytic and electrocatalytic applications, hydrazone-linked COFs could also bring non-negligible possibilities in chemical catalysis. However, so far, there are only a limited number of hydrazone-linked COFs that are applied for chemical catalysis, including selective oxidation reaction, tandem reaction and chlorobenzenes (CBs) dichlorination. In 2014, a molybdenum-doped COF catalyst (Mo-COF) was synthesized *via* a bottom-up approach for catalyzing the reaction of selective oxidation.[13] As a result, the Mo-COF performed well (＞99% conversion and 71% selectivity) as an open nanochannel-reactor for catalyzing the reaction of epoxidation of cyclohexene. Besides, Chen et al. reported a heteroatomic hydrazone-linked COF-ASB (1) that can upload Ru nanoparticles to produce Ru@COF-ASB (2).[21] Under solvent-free conditions, the obtained material could highly facilitate the tandem synthesis reactions for the production of imines through the coupling reaction of benzyl alcohols and amines (conversion 90%, selectivity 100%). Moreover, Dong et al. loaded Pd nanoparticles onto an allyl-decorated hydrazone-linked COF-AO (1) to generate Pd@COF-AO (2) (Figure 18a).[56] A uniform, water permeable and elastic membrane 3 was prepared by incorporating 2 with thiol-functionalized polysiloxane through click reaction and it can be used as a micro-environment for catalyzing the dechlorination reaction of CBs. Within 3 h at room temperature, Pd@COF-AO (2) could catalyze the transformation of phenol from p-chlorophenol with >99% yield (Figure 18b). Even after five cycles, it still showed remained catalytic activity (Figure 18c). Moreover, the authors constructed a continuous-flow device for a continuous catalytic process of the dechlorination of p-chlorophenol considering the merit of the porous membrane 3.

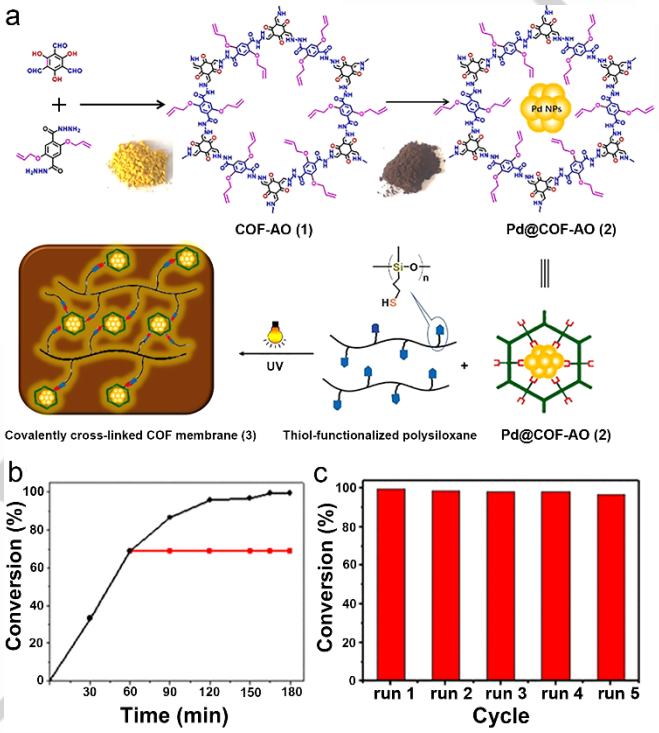


***Figure 18.*** Schematic representation of COF-AO (1), Pd@COF-AO (2) and relative p-chlorophenol dehalogenation performance. a) Synthesis route of COF-AO (1), Pd@COF-AO (2) and their COF-based membrane (3). b) Catalytic performance (the black line represented reaction time test while the red line represented leaching test). c) Catalytic cycles. Reproduced with permission.[56] Copyright 2018, American Chemical Society.

### 3.4. Chemical sensing

Chemical sensing is an important method for detecting ions and some pollutants.[57] Hydrazone-linked COFs have porous and flexible structures with designable active sites, making them a candidate material for chemical sensing. From a structure perspective, the regularly aligned channels of hydrazone-linked COFs are beneficial for the interaction between contact active sites and target substances. Moreover, hydrazone-linked COFs exhibit exceptional hydrolytic stability that can preserve the integrity of structure after sensing test. In this section, we will divide the contents of chemical sensing into ion sensing, pH sensing and water sensing, etc.

### 3.4.1. Ion sensing

With the discharge of industrial wastewater, an increasing number of hazardous ions have been released into the environment, endangering human health and livelihood.[58]

10.1002/anie.202404941



Among these ions, Cr, Cu and Hg ions are common heavy metal ions around us and once absorbed, they will aggregate within the organism and cause irreversible damage. Thus, it's crucial to develop high-performance sensing materials that can detect these toxic ions.[59] To this end, the hydrazone-linked COFs are promising sensing candidates owing to their multiple active N/O sites that could coordinate with metal ions. For example, in 2019, a highly luminescent pyrene-based hydrazone-linked COF (TFPPy-CHYD) was created and featured a 17 nM detection limit for mercury (Figure 19a).[60] Significantly, TFPPy-CHYD showed outstanding adsorption capacities of $Hg^0$ (232 mg $g^{-1}$) and $Hg^{2+}$ (758 mg $g^{-1}$) in both air and water, respectively (Figure 19b-c). Amides with side chains also show an important role in sensing. For example, a hydrazone-linked COF-LZU8 possessing thioether groups was rationally prepared for $Hg^{2+}$ sensing.[61] Notably, it displayed a low detection limit for $Hg^{2+}$ (25.0 ppb) due to its hydrazone linkage with high stability, well-distributed thioether groups and uniform pore channels.

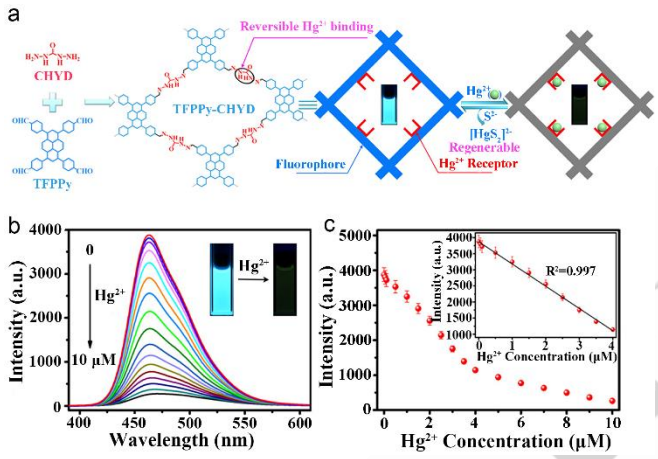


***Figure 19.*** Synthesis and sensing performance of TFPPy-CHYD COF a) Schematic representation for $Hg^{2+}$ sensing. b) Fluorescence emission spectra. c) The plot of fluorescence intensity (463 nm) and $Hg^{2+}$ concentration. Reproduced with permission.[60] Copyright 2020, American Chemical Society.

Apart from the removal of $Hg^{2+}$, the sensing of $Fe^{3+}$ was also broadly explored. For example, an NCD@COF BTT-Th nanosheet was prepared with the encapsulation of N-doped carbon dots (NCDs) into the pore channels and displayed strong dual-emission.[62] It was worth mentioning that NCD@COF BTT-Th exhibited a 3.40 nM detection limit for $Fe^{3+}$, which might be ascribed to the possible energy transfer that existed in NCDs and COF BTT-Th. In addition, a hydrazone-linked Bth-Dma COF with post-chelating sites was rationally designed for detecting $Fe^{3+}$.[63] Notably, the Bth-Dma COF displayed strong fluorescence and sensing ability. When used for $Fe^{3+}$ sensing, it exhibited a 0.17 μM detection limit, which could be ascribed to the coordination ability between $Fe^{3+}$ and the chelating sites. Furthermore, Xia et al. successfully synthesized two kinds of COF-based paper composites (COF-Paper1 and COF-Paper2) with exceptional solid-state luminescence *via* an in-situ growth method.[64] Interestingly, they could be employed as turn-off fluorescence sensors for detecting $Fe^{3+}$ and $UO_2^{2+}$ visually. Significantly, it demonstrated a low sensing limit (5.6 ng $cm^{-2}$ for $Fe^{3+}$ and 27 ng $cm^{-2}$ for $UO_2^{2+}$). Additionally, another novel stable Tfpa-Mth COF was synthesized and uniformly dispersed in ethanol.[65] When employed as a fluorescence sensor for detecting $Fe^{3+}$, Tfpa-Mth COF demonstrated a low detection limit of 64 nM and high selectivity. Moreover, growing Tfpa-Mth COF on a quartz crystal microbalance (QCM) chip, a kind of COF-based QCM sensor was prepared and employed to monitor $Fe^{3+}$.[65] The QCM sensor is capable of monitoring $Fe^{3+}$, which might facilitate the development of COF-based sensing devices for detecting metal ion.

Besides, the detection of other ions ($Cu^{2+}$, $Pd^{2+}$ and $F^-$) was also investigated. For example, a hydrazone-linked COF (TFB-BMTH) was successfully synthesized and used as a sensor for $Cu^{2+}$ detection.[44g] When adding 0.1 mM $Cu^{2+}$ into the suspension of TFB-BMTH within 10 s, apparent fluorescence quenching (90%) was detected with largely reduced fluorescence quantum yield (5.79% to 1.33%), which could be ascribed to the charge transfer from the ligands to $Cu^{2+}$ owing to the coordination between $Cu^{2+}$ and the binding sites (N/O atoms). In addition, a hydrazone-linked COF (XB-COF) with the modification of the allyl group was proposed for the selective fluorescent detection of $Pd^{2+}$.[66] XB-COF displayed good stability achieved by hydrazone linkage and good complexation ability to $Pd^{2+}$ with the presence of allyl. Therefore, XB-COF showed good fluorescence response and high adsorption capacity for $Pd^{2+}$ (120 mg $g^{-1}$). Nonetheless, the bulk powder form of the reported hydrazone-linked COFs still presented a limited sensing ability, especially for the accessibility of substrates to active sites. Therefore, some works exfoliated hydrazone-linked COFs into 2D morphology like nanosheets to enhance their sensing ability. Given this, Singh et al. had designed and synthesized a self-exfoliable iCONs ($DATG_{Cl}$-iCONs) for the sensing of $F^-$.[67] It was demonstrated that $DATG_{Cl}$-iCONs displayed a sensing limit of 5 ppb for $F^-$. The high performance may be ascribed to the well-exposed active sites and cationic properties in the structure.

### 3.4.2 Other sensing applications

Except for the sensing of toxic ions, hydrazone-linked COFs are also used for the detection of other substances, such as enrofloxacin, trace water, dopamine, acid vapor, and so on. For instance, the fluorescence property of BTT-based hydrazone-linked COFs (i.e., $COF_{BTT\text{-}H}$, $COF_{BTT\text{-}DGMH}$ and $COF_{BTT\text{-}TAGH}$) could be regulated by the tuning of amine monomers.[19] Furthermore, they could be fabricated in the form of test paper and gel. Combined with an RGB analysis of smartphone applications, this test paper and gel were effectively applied for the detection of enrofloxacin in fish or clam metabolite. The detection limits were achieved 106.2 nM and 26.00 nM in test paper and gel real-time detection devices, respectively. Additionally, a hydrazone-linked BTA-COF was modified by $Cu^{2+}$ and employed for triple-mode dopamine sensing.[68] After adding $H_2O_2$ and 1,3-dihydroxynaphthalene, the Cu-BTA-COF could sensitively and selectively detect the dopamine. Specifically, it displayed 7.2, 8.6, and 23 nM detection limits for dopamine sensing through fluorescence, colorimetry and smartphone modes, respectively. Moreover, it enabled gratifying recoveries (97.6-100.4%) for dopamine detection in human urine samples under three modes. Except for detecting enrofloxacin and dopamine, the detection of trace water is highly important for ultra-dry reagents and ultra-dry experiment operation, which are closely related to the purity and yield of products.[69] Given this, hydrazone-linked Pythz-COF and urea-linked Pyurea-COF were proposed and employed as scaffolds for the harvesting of water vapor and sensing of trace water.[70]

Remarkably, Pythz-COF and Pyurea-COF displayed a 0.09% and 0.02% sensing detection limit for the detection of trace water in acetonitrile, respectively. Moreover, they also displayed high cycling stability even after five cycles.

Except for the sensing of enrofloxacin, dopamine and trace water, other applications of hydrazone-linked COFs focused on pH or acid vapor sensing have been reported. For instance, a hydrazone-linked COF-JLU4 featured outstanding hydrolytic stability was applied as pH sensing.[71] Remarkably, COF-JLU4 displayed a wide pH-dependent fluorescence response in aqueous solutions (pH, 0.9 - 13). This finding indicated the utility of the hydrazone-linked COFs in pH-sensing and would extend the application aspects of hydrazone-linked COFs. For acid vapor sensing, Gong et al. constructed two hydrazone-linked COFs (TPE-DHZ-COF and TPB-DHZ-COF) with TPE unit owning an aggregation-induced emission (AIE).[72] TPE-DHZ-COF showed superior luminescence properties to TPB-DHZ-COF, indicating the solid-state luminescence performance can be enhanced by imparting AIE-active units in hydrazone-linked COFs. These results demonstrated that hydrazone-linked COFs might hold much potential for fluorescence sensing.

### 3.5. Energy storage

Energy storage is currently a very emerging field and hydrazone-linked COFs have arisen to be a promising candidate of energy storage materials. So far, it can be used as a SEs, electrode material, and membrane modification for lithium/Zn-air/Na-S batteries. In the following part, we will discuss each section in detail.

The investigation of $Li^+$ conducting in solid phase is vital for the construction of efficient solid-state lithium batteries. In 2018, Chen's group for the first time introduced a cationic skeleton into the hydrazone-linked COF skeleton (CON-Cl) for the study of $Li^+$ conducting (Figure 20a).[73] It is detected that the $Li^+$ conductivity ($2.09 \times 10^{-4}$ S $cm^{-1}$ at 70 °C) in the absence of any solvent could be largely improved by increasing the free $Li^+$ concentration through the splitting of ion pair of Li salt (Figure 20b-e). In addition, SEs is an important component for designing high energy density and safe batteries. In 2020, Li et al. constructed a lithiated hydrazone-linked COF (LiCON-3) as an SEs with integrated phenol and allyl groups in the pore structure.[7a] It achieved a $10^{-5}$ S $cm^{-1}$ $Li^+$ conductivity of at 233 K with a $Li^+$ transference number (0.92). When coupled with 1,4-benzoquinone cathode, the battery applying LiCON-3 as a SEs could run for 500 cycles (500 mA $g^{-1}$) at 293 K.

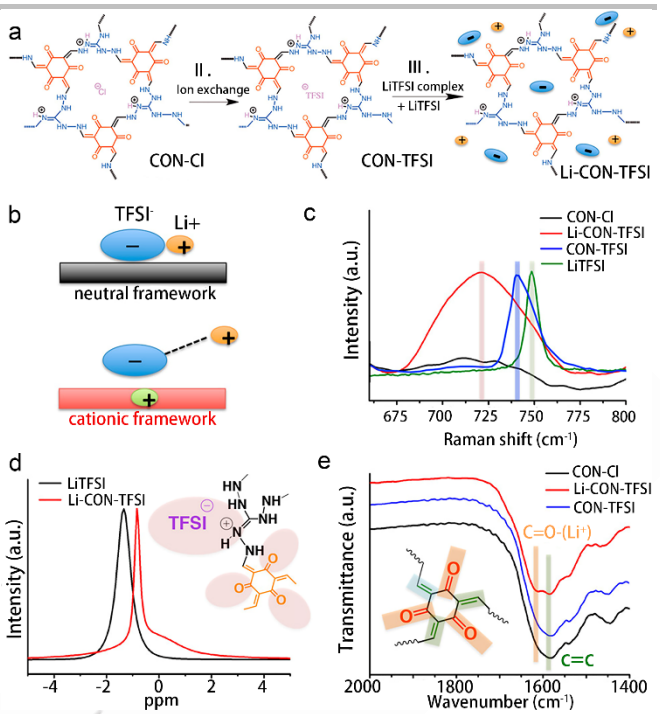


***Figure 20.*** Synthesis and characterization of Li-CON-TFSI. a) Synthetic route. b) Schematic diagram of the ion pair. c) Raman spectra. d) $^7$Li MAS NMR spectra. e) FTIR spectra. Reproduced with permission.[73] Copyright 2018, American Chemical Society.

It is essential for developing proton conducting materials in fuel batteries.[74] In this regard, Wu et al. constructed three hydrazone-linked COFs (i.e., COF-F6, COF-F8 and COF-F10) and explored their performances with varying fluorine chains.[75] Notably, compared to their nonfluorous counterparts, fluorinated COFs exhibited a high proton conductivity ($4.2 \times 10^{-2}$ S $cm^{-1}$ at 140 °C) with the doping of $H_3PO_4$ owing to the superhydrophobic channels could act as a scaffold to encapsulate numerous phosphonic acid for high-performance proton conduction. In addition, Jiang's group fabricated a range of QA-functionalized hydrazone-linked COF membranes (COF-QAs) for anion conduction.[76] Interestingly, COF-QAs membranes achieved high hydroxide ion conductivity (200 mS $cm^{-1}$ at 80 °C, 100% RH) owing to well-ordered pore channels and QA function groups. Except for the ion conduction, hydrazone-linked COFs are also employed as battery electrode materials. For example, Li et al. used a hydrazone/hydrazide-containing COF for cathode materials of Li-$CO_2$ battery.[77] Owing to the robust pore channels in the structure that could serve as $Li^+$ and $CO_2$ diffusion channels, the battery showed a high capacity (27348 mAh $g^{-1}$ at 200 mA $g^{-1}$) and a cut-off overpotential (1.24 V) at 1000 mAh $g^{-1}$. Moreover, hydrazone-linked COFs can be used as a coating to modify the separator. Recently, Liu et al. designed a cationic hydrazone-linked COF (COF-F) possessing units with a positive charge and $F^-$ and served as a coating for the PP separator.[78] It was demonstrated that the COF-F@PP-based batteries exhibited an 18 mV overpotential owing to the loosely bonded $F^-$ that is profit to form LiF-riched SEI, lower than that of COF-Cl@PP-based batteries (27 mV) and pristine PP-based batteries (31 mV). Moreover, Zhang et al. prepared a fluorinated hydrazone-linked COFs (4F-COF)-based membrane.[79] As a result, Li symmetrical batteries

10.1002/anie.202404941



with 4F-COF/PP separator showed exceptional cycle stability (2000 h at 1 mA $cm^{-2}$). Meanwhile, lithium-sulfur batteries with 4F-COF/PP separator achieved an 82.3% cycling retention over 1000 cycles at 2 C and 568.0 mA h $g^{-1}$ rate performance at 10 C.

In addition to lithium batteries, hydrazone-linked COFs are also employed as Zn-air battery electrodes. In general, hydrazone-linked COFs exist in powder form, however, films are more processable in comparison to powders. In this regard, Jiang et al. reported a serial of metalloporphyrin-based hydrazone-linked COF (CoP-TOB) films and explored their applications for Zn-air batteries.[8c] Notably, using the CoP-TOB films, a flexible all-solid-state Zn-air battery was created, displaying good performance with a 0.88 V charge-discharge voltage gap at 1 mA $cm^{-2}$. Sodium-sulfur batteries based on hydrazone-linked COFs were also investigated. For example, Wang et al. synthesized a hydrazone-linked COFs (Azo-TbTh) film with azobenzene branches (Figure 21a-b).[80]. Exceptionally, the batteries with Azo-TbTh-equipped separators exhibited an extremely low decay rate (0.036% per cycle) over 1000 cycles at 1 C (Figure 21d), which is attributed to the dual functions of azobenzene branches: preventing the shuttle of polysulfide and act as $Na^+$ migration ion-hopping sites (Figure 21c).

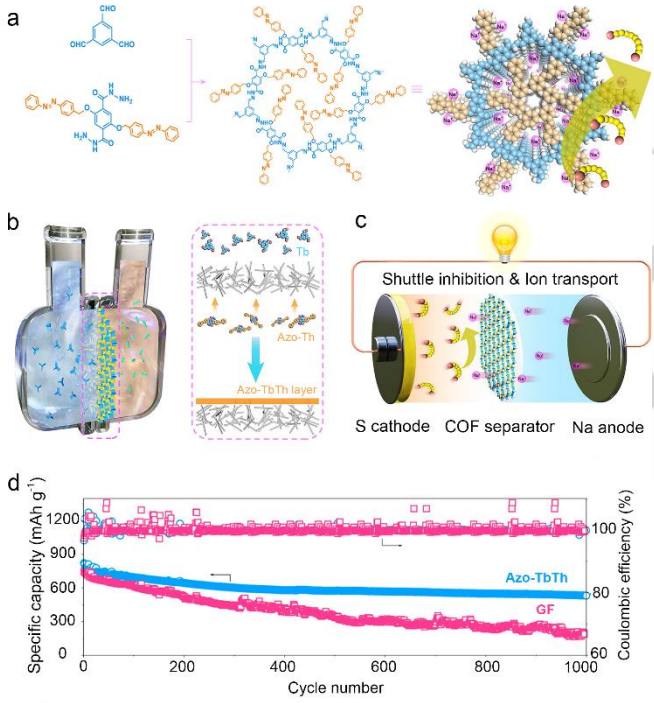


***Figure 21.*** Synthesis and battery performance of Azo-TbTh COF. a) Synthetic Figure of the Azo-TbTh COF. b) Synthetic representation of the polymerization of COF film. c) Schematic diagram of the batteries based on Azo-TbTh-equipped separators for fast $Na^+$ transport and blocking of polysulfide. d) Cycle performance. Reproduced with permission.[80] Copyright 2022, American Chemical Society.

## 4. Perspectives

Since the first report in 2011, a series of intriguing characteristics and applications of hydrazone-linked COFs have been developed based on their superior characteristics. They are rising stars in Schiff-base COFs, which originates from the inherent nature of Schiff-base COFs meanwhile possessing unique properties by themselves. Based on the reported works to date, their main characteristics can be mainly summarized: structural flexibility, heteroatom sites, post-modification ability and hydrolytic stability. These characteristics endow hydrazone-linked COFs with much potential in diverse application fields like adsorption/separation, catalysis, chemical sensing and energy storage, etc. Although many applications have been achieved by hydrazone-linked COFs, there are still some significant issues that need to be carefully addressed: 1) the aromatic hydrazine monomers are hard to solute in common organic solvents and their flexible backbones would hinder the π-π stacking effect to result in low crystallinity; 2) more ligands would be still needed to enrich the diversity of hydrazone-linked COFs; 3) the preparation methods that can be processed under milder conditions and ease in scale-up production are desired; 4) most of the reported hydrazone-linked COFs are in powder forms and facilely processible devices like films, membranes, fibers or foams are still rare; 5) their specific characteristics need to be fully utilized and extended to more relevant applications to reveal their superiority and 6) the structure-to-property relationships of hydrazone-linked COFs are essential for the detailed mechanistic study yet some of reported works are still missing.

Thus, further investigations of hydrazone-linked COFs should pay more attention to some important issues: 1) for the syntheses of hydrazone-linked COFs with high crystallinity, it would be necessary to add substituent groups to promote the dissolution of structural units or strengthen the π-π stacking to produce highly crystalline hydrazone-linked COFs; 2) for the variety of hydrazone-linked COFs, more complex ligands with diverse functions need to be explored for the enrichment of their synthesis methology; 3) for the milder preparation methods, we need to develop facile hydrazone-linked COFs systems that can be readily prepared under air or lower temperatures, and advanced synthesis techniques like ultrasound, microwave, high-throughput or GPT-4; 4) for the processible devices, hydrazone-linked COFs based stand-alone or composite films, membranes, fibers or foams would need more research works to facilitate their lab-to-industry process; 5) for their unique characteristics like the structural flexibility, heteroatom sites, post-modification ability and hydrolytic stability, directional applications that can fully utilize these characteristics would be much demanded to maximize the advantages of hydrazone-linked COFs and 6) for the mechanistic study, more detailed and deeper investigation would be needed to extend the potential of hydrazone-linked COFs, so as to directionally guide the syntheses of hydrazone-linked COFs.

## 5. Summary

In this review, we systematically review the recent progress of hydrazone-linked COFs. Initially, we present basic information about hydrazone-linked COFs including their design, characteristics and preparation methods. After that, we focus on the applications of hydrazone-linked COFs, including adsorption/separation, catalysis, chemical sensing and energy storage, and discuss their structure-to-property relationships. Finally, we present a perspective on their challenges and opportunities. We hope that this review would give readers new insights about hydrazone-linked COFs and inspire scientists to explore more appealing functions or applications for the future development of hydrazone-linked COFs.

## Acknowledgements

This work was financially supported by the National Key R&D Program of China (2023YFA1507204). National Natural Science Foundation of China (Grants 22171139, 22225109, 22071109). Natural Science Foundation of Guangdong Province (No. 2023B1515020076).

**Keywords:** Covalent Organic Frameworks • Hydrazone Linkage • Structural flexibility • Hydrolytic stability • Heteroatomic sites

[1] a) X. Chen, K. Geng, R. Liu, K. T. Tan, Y. Gong, Z. Li, S. Tao, Q. Jiang, D. Jiang, *Angew. Chem., Int. Ed.* **2019**, *59*, 5050-5091; b) X. Guan, F. Chen, S. Qiu, Q. Fang, *Angew. Chem., Int. Ed.* **2022**, *62*, e202213203 ; c) H. Guo, D. H. Si, H. J. Zhu, Z. A. Chen, R. Cao, Y. B. Huang, *Angew Chem Int Ed Engl* **2024**, *63*, e202319472; d) N. Huang, P. Wang, D. Jiang, *Nat. Rev. Mater.* **2016**, *1*, 16068; e) W. Zhang, L. Chen, S. Dai, C. Zhao, C. Ma, L. Wei, M. Zhu, S. Y. Chong, H. Yang, L. Liu, Y. Bai, M. Yu, Y. Xu, X.-W. Zhu, Q. Zhu, S. An, R. S. Sprick, M. A. Little, X. Wu, S. Jiang, Y. Wu, Y.-B. Zhang, H. Tian, W.-H. Zhu, A. I. Cooper, *Nature* **2022**, *604*, 72-79.

[2] a) Y. R. Wang, H. M. Ding, X. Y. Ma, M. Liu, Y. L. Yang, Y. Chen, S. L. Li, Y. Q. Lan, *Angew. Chem., Int. Ed.* **2021**, *61*, e202114648 ; b) R. Xu, D. H. Si, S. S. Zhao, Q. J. Wu, X. S. Wang, T. F. Liu, H. Zhao, R. Cao, Y. B. Huang, *J Am Chem Soc* **2023**, *145*, 8261-8270; c) X. Yao, C. Guo, C. Song, M. Lu, Y. Zhang, J. Zhou, H. M. Ding, Y. Chen, S. L. Li, Y. Q. Lan, *Adv. Mater.* **2022**, *35*, 2208846; d) J. Zhou, J. Li, L. Kan, L. Zhang, Q. Huang, Y. Yan, Y. Chen, J. Liu, S.-L. Li, Y.-Q. Lan, *Nat. Commun.* **2022**, *13*, 4681; e) H. J. Zhu, D. H. Si, H. Guo, Z. Chen, R. Cao, Y. B. Huang, *Nat Commun* **2024**, *15*, 1479.

[3] a) A. P. Coˆte´, A. I. Benin, N. W. Ockwig, M. O'Keeffe, A. J. Matzger, O. M. Yaghi, *Science* **2005**, *310*, 1166-1170; b) S. Dalapati, S. Jin, J. Gao, Y. Xu, A. Nagai, D. Jiang, *J. Am. Chem. Soc.* **2013**, *135*, 17310-17313; c) Q. Fang, Z. Zhuang, S. Gu, Y. Yan, *Nat. Commun.* **2014**, *5*, 4503; d) J. Guo, Yanhong, S. Jin, L. Chen, T. Kaji, Y. Honsho, M. A. Addicoat, J. Kim, A. Saeki, H. Ihee, S. Seki, S. Irle, M. Hiramoto, J. Gao, D. Jiang, *Nat. Commun.* **2013**, *4*, 2736; e) S. Kandambeth, A. Mallick, B. Lukose, M. V. Mane, T. Heine, R. Banerjee, *J. Am. Chem. Soc.* **2012**, *134*, 19524-19527; f) P. Kuhn, M. Antonietti, A. Thomas, *Angew. Chem., Int. Ed.* **2008**, *47*, 3450-3453; g) D. Kurandina, B. Huang, W. Xu, N. Hanikel, K. Wang, F. D. Toste, O. M. Yaghi, *Angew. Chem., Int. Ed.* **2023**, *62*, e202307674; h) A. Nagai, X. Chen, X. Feng, X. Ding, Z. Guo, D. Jiang, *Angew. Chem., Int. Ed.* **2013**, *52*, 3770-3774; i) F. J. Uribe-Romo, C. J. Doonan, H. Furukawa, K. Oisaki, O. M. Yaghi, *J. Am. Chem. Soc.* **2011**, *133*, 11478-11481; j) F. J. Uribe-Romo, J. R. Hunt, H. Furukawa, C. Klöck, M. O'Keeffe, O. M. Yaghi, *J. Am. Chem. Soc.* **2008**, *131*, 4570; k) B. Zhang, M. Wei, H. Mao, X. Pei, S. A. Alshmimri, J. A. Reimer, O. M. Yaghi, *J. Am. Chem. Soc.* **2018**, *140*, 12715-12719; l) C. Zhao, H. Lyu, Z. Ji, C. Zhu, O. M. Yaghi, *J. Am. Chem. Soc.* **2020**, *142*, 14450-14454; m) X. Zhuang, W. Zhao, F. Zhang, Y. Cao, F. Liu, S. Bia, X. Feng, *Polym. Chem.* **2016**, *7*, 4176-4181.

[4] J. Segura, M. Manchen, F. Zamora, *Chem. Soc. Rev.* **2016**, *45*, 5635-5671.

[5] a) X. Li, Q. Gao, J. Wang, Y. Chen, Z. H. Chen, H.-S. Xu, W. Tang, K. Leng, G.-H. Ning, J. Wu, Q.-H. Xu, S. Y. Quek, K. P. Loh, *Nat. Commun.* **2018**, *9*, 2335; b) Y. Li, J. Sui, L.-S. Cui, H.-L. Jiang, *J. Am. Chem. Soc.* **2023**, *145*, 1359-1366; c) Z. B. Zhou, H. H. Sun, Q. Y. Qi, X. Zhao, *Angew. Chem., Int. Ed.* **2023**, *62*, e202305131.

[6] Y. He, Y. Zhao, X. Wang, Z. Liu, Y. Yu, L. Li, *Angew. Chem., Int. Ed.* **2023**, *62*, e202307160.

[7] a) X. Li, Q. Hou, W. Huang, H.-S. Xu, X. Wang, W. Yu, R. Li, K. Zhang, L. Wang, Z. Chen, K. Xie, K. P. Loh, *ACS Energy Lett.* **2020**, *5*, 3498-3506; b) Y. Yan, X. Li, G. Chen, K. Zhang, X. Tang, S. Zhang, S. Zheng, J. Fan, W. Zhang, S. Cai, *Chinese Chem. Lett.* **2021**, *32*, 107-112; c) S. Yang, Z. Chen, L. Zou, R. Cao, *Adv. Sci.* **2023**, *10*, 2304697.

[8] a) D. N. Bunck, W. R. Dichtel, *J. Am. Chem. Soc.* **2013**, *135*, 14952-14955; b) R.-R. Liang, R.-H. A, S.-Q. Xu, Q.-Y. Qi, X. Zhao, *J. Am. Chem. Soc.* **2020**, *142*, 70-74; c) J. Tang, Z. Liang, H. Qin, X. Liu, B. Zhai, Z. Su, Q. Liu, H. Lei, K. Liu, C. Zhao, R. Cao, Y. Fang, *Angew. Chem., Int. Ed.* **2022**, *62*, e202214449.

[9] a) Y. Ge, J. Li, Y. Meng, D. Xiao, *Nano Energy* **2023**, *109*, 108297; b) X. Liu, J. Li, B. Gui, G. Lin, Q. Fu, S. Yin, X. Liu, J. Sun, C. Wang, *J. Am. Chem. Soc.* **2021**, *143*, 2123-2129.

[10] a) S. Bi, Z. Zhang, F. Meng, D. Wu, J. S. Chen, F. Zhang, *Angew. Chem., Int. Ed.* **2021**, *61*, e202111627; b) D. Li, C. Li, L. Zhang, H. Li, L. Zhu, D. Yang, Q. Fang, S. Qiu, X. Yao, *J. Am. Chem. Soc.* **2020**, *142*, 8104-8108; c) M. Liu, S. Liu, C. X. Cui, Q. Miao, Y. He, X. Li, Q. Xu, G. Zeng, *Angew. Chem., Int. Ed.* **2022**, *61*, e202213522

[11] Y. Yusran, J. Xing, Q. Lin, G. Wu, W.-C. Peng, Y. Wu, T. Su, L. Yang, L. Zhang, Q. Li, H. Wang, Z.-T. Li, D.-W. Zhang, *Small* **2023**, *19*, 2303069

[12] Y. Li, X. Guo, X. Li, M. Zhang, Z. Jia, YunDeng, Y. Tian, S. Lia, L. J. Ma, *Angew. Chem., Int. Ed.* **2020**, *59*, 4168-4175.

[13] W. Zhang, P. Jiang, Y. Wang, J. Zhang, Y. Gao, P. Zhang, *RSC Adv.* **2014**, *4*, 51544-51547.

[14] Y.-X. Yang, X.-H. Tang, J.-L. Wu, Z.-Y. Dong, Y.-L. Yan, S.-R. Zheng, J. Fan, X. Li, S. Cai, W.-G. Zhang, *ACS Appl. Polym. Mater.* **2022**, *4*, 4624-4631.

[15] S. Yang, H. Lv, H. Zhong, D. Yuan, X. Wang, R. Wang, *Angew. Chem., Int. Ed.* **2022**, *61*, e202115655.

[16] M. Yang, F. Qiu, E.-S. M. El-Sayed, W. Wang, S. Du, K. Su, D. Yuan, *Chem. Sci.* **2021**, *12*, 13307-13315.

[17] A. Ajnsztajn, V. V. J. Harikrishnan, S. B. Alahakoon, D. Zhu, M. Barnes, J. Daum, J. Gayle, G. Tomur, J. Lowenstein, S. Roy, P. M. Ajayan, R. Verduzco, *Chemistry* **2023**, *29*, e202302304.

[18] J.-Y. Dai, Y.-X. Fang, Z.-L. Xu, D. Pandaya, J. Liang, H.-F. Yan, Y.-J. Tang, *Desalination* **2023**, *568*, 117025.

[19] L. Yang, M. Li, L. Kuang, Y. Li, L. Chen, C. Lin, L. Wang, Y. Song, *Biosens Bioelectron.* **2022**, *214*, 114527.

[20] X. Zhuang, J. Hao, X. Zheng, D. Fu, P. Mo, Y. Jin, P. Chen, H. Liu, G. Liu, W. Lv, *Sep. Purif. Technol.* **2021**, *274*, 118993.

[21] G.-J. Chen, X.-B. Li, C.-C. Zhao, H.-C. Ma, J.-L. Kan, Y.-B. Xin, C.-X. Chen, Y. B. Dong, *Inorg. Chem.* **2018**, *57*, 2678-2685.

[22] G. Das, D. B. Shinde, S. Kandambeth, B. P. Biswal, R. Banerjee, *Chem. Commun.* **2014**, *50*, 12615-12618.

[23] Z. Guo, H. Jiang, H. Wu, L. Zhang, S. Song, Y. Chen, C. Zheng, Y. Ren, R. Zhao, Y. Li, Y. Yin, M. D. Guiver, Z. Jiang, *Angew. Chem., Int. Ed.* **2021**, *60*, 27078-27085.

[24] J. P. Daum, A. Ajnsztajn, S. A. Iyengar, J. Lowenstein, S. Roy, G. H. Gao, E. H. R. Tsai, P. M. Ajayan, R. Verduzco, *ACS Nano* **2023**, *17*, 21411-21419.

[25] a) X. Li, Q. Shi, M. Li, N. Song, Y. Xiao, H. Xiao, T. D. James, L. Feng, *Chinese Chem. Lett.* **2023**, 109021; b) G. L. Yang, X. L. Jiang, H. Xu, B. Zhao, *Small* **2021**, *17*, 2005327; c) C. Zhao, G. Liu, Q. Tan, M. Gao, G. Chen, X. Huang, X. Xu, L. Li, J. Wang, Y. Zhang, D. Xu, *J. Adv. Res.* **2023**, *44*, 53-70.

[26] Y. An, W. Zhang, X. Zhang, Y. Zhong, L. Ding, Y. Hao, M. White, Z. Chen, Z. An, X. Wang, *Langmuir* **2023**, *39*, 12324.

[27] S. Jansone-Popova, A. Moinel, J. A. Schott, S. M. Mahurin, I. Popovs, G. M. Veith, B. A. Moyer, *Environ. Sci. Technol.* **2019**, *53*, 878-883.

[28] Y. Li, C. Wang, S. Ma, H. Zhang, J. Ou, Y. Wei, M. L. Ye, *ACS Appl. Mater. Interfaces* **2019**, *11*, 11706-11714.

[29] L. Zhang, Y. Li, Y. Wang, S. Ma, J. Ou, Y. Shen, M. Ye, H. Uyama, *J. Hazard. Mater.* **2021**, *407*, 124390.

[30] H.-J. Da, C.-X. Yang, X. P. Yan, *Environ. Sci. Technol.* **2019**, *53*, 5212-5220.

[31] J. Yu, J. Lan, S. Wang, P. Zhang, K. Liu, L. Yuan, Z. Chai, *Dalton Trans.* **2021**, *50*, 3792-3796.

[32] H.-J. Da, C.-X. Yang, H.-L. Qian, X.-P. Yan, *J. Mat. Chem. A* **2020**, *8*, 12657-12664.

[33] a) T. Liu, Y. Zhao, M. Song, X. Pang, X. Shi, J. Jia, L. Chi, G. Lu, *J. Am. Chem. Soc.* **2023**, *145*, 2544-2552; b) Y. Xie, T. Pan, Q. Lei, C. Chen, X. Dong, Y. Yuan, W. A. Maksoud, L. Zhao, L. Cavallo, I. Pinnau, Y. Han, *Nat. Commun.* **2022**, *13*, 2878; c) J. Zhang, J. Liu, Y. Liu, Y. Wang, Q. Fang, S. Qiu, *Chem. Res. Chinese U.* **2022**, *38*, 456-460.

[34] a) K. Cheng, H. Li, Z. Li, P.-Z. Li, Y. Zhao, *ACS Materials Lett.* **2023**, *5*, 1546-1555; b) H. Li, D. Zhang, K. Cheng, Z. Li, P.-Z. Li, *ACS Appl. Nano Mate.* **2023**, *6*, 1295-1302.

[35] Z. Zhang, X. Dong, J. Yin, Z.-G. Li, X. Li, D. Zhang, T. Pan, Q. Lei, X. Liu, Y. Xie, F. Shui, J. Li, M. Yi, J. Yuan, Z. You, L. Zhang, J. Chang, H. Zhang, W. Li, Q. Fang, B. Li, X.-H. Bu, Y. Han, *J. Am. Chem. Soc.* **2022**, *144*, 6821-6829.

[36] S.-Y. Zhang, X.-H. Tang, Y.-L. Yan, S.-Q. Li, S. Zheng, J. Fan, X. Li, W.-G. Zhang, S. L. Cai, *ACS Macro. Lett.* **2021**, *10*, 1590-1596.

[37] N. Bagherian, A. R. Karimi, A. A. b, *Colloid. Surfaces A* **2021**, *613*, 126078.

[38] M. Zhang, R. Zheng, Y. Ma, R. Chen, X. Sun, X. Sun, *Micropor. Mesopor. Mat.* **2019**, *285*, 70-79.

[39] K. Gottschling, L. Stegbauer, G. k. Savasci, N. A. Prisco, Z. J. Berkson, C. Ochsenfeld, B. F. Chmelk, B. V. Lotsch, *Chem. Mater.* **2019**, *31*, 1946-1955.

[40] L. Zhang, L. Wang, N. Wang, H. Guo, W.-H. Zhang, X. Li, S. Ji, Q.-F. An, *J. Mem. Sci.* **2020**, *598*, 117652.

[41] K. Zhang, S.-L. Cai, Y.-L. Yan, Z.-H. He, H.-M. Lin, X.-L. Huang, S.-R. Zheng, J. Fan, W.-G. Zhang, *J. Chromatogr. A* **2017**, *1519*, 100-109.

[42] W. Lv, Y. Zhang, G. Wang, L. Zhao, F. Wang, Y. Chen, H. Chen, X. Zhang, X. Chen, *J. Chromatogr. A* **2022**, *1677*, 463289.

[43] a) J.-N. Chang, J.-W. Shi, Q. Li, S. Li, Y.-R. Wang, Y. Chen, F. Yu, S.-L. Li, Y.-Q. Lan, *Angew. Chem., Int. Ed.* **2023**, *62*, e202303606 ; b) M. Lu, M. Zhang, J. Liu, T.-Y. Yu, J.-N. Chang, L.-J. Shang, S.-L. Li, Y.-Q. Lan, *J. Am. Chem. Soc.* **2022**, *144*, 1861; c) H. Li, L. Wang, G. Yu, *Nano Today* **2021**, *40*, 101247.

[44] a) W. Qi, K. Luo, Q. Su, X. Sun, X. Li, Z. Liu, Q. Wu, *Catal. Lett.* **2022**, *153*, 2331; b) S. Liu, W. Pan, S. Wu, X. Bu, S. Xin, J. Yu, H. Xu, X. Yang, *Green Chem.* **2019**, *21*, 2905-2910; c) Q. wu, W. Liu, Q. Su, P. Ju, B. Guo, H. Zhou, G. Li, *ChemSusChem* **2017**, *10*, 664-669; d) M. Tian, S. Liu, X. Bu, J. Yu, X. Yang, *Chem. Eur. J.* **2020**, *26*, 369-373; e) M.-H. Li, Z. Yang, Z. Li, J.-R. Wu, B. Yang, Y.-W. Yang, *Chemistry of Materials* **2022**, *34*, 5726-5739; f) Z. Liu, Q. Su, P. Ju, X. Li, G. Li, Q. Wu, B. Yang, *Chem. Commun.* **2020**, *56*, 766-769; g) S. Liu, Z. Liu, Q. Su, Q. Wu, *Micropor. Mesopor. Mat.* **2022**, *333*, 111737.

10.1002/anie.202404941






[45] a) X. Guan, Y. Qian, X. Zhang, H.-L. Jiang, *Angew. Chem., Int. Ed.* **2023**, *62*, e202306135 ; b) F.-M. Zhang, J.-L. Sheng, Z.-D. Yang, X.-J. Sun, H.-L. Tang, M. Lu, H. Dong, F.-C. Shen, J. Liu, Y.-Q. Lan, *Angew. Chem., Int. Ed.* **2018**, *57*, 12106.

[46] L. Stegbauer, K. Schwinghammer, B. V. Lotsch, *Chem. Sci.* **2014**, *5*, 2789-2793.

[47] K. Gottschling, G. k. Savasci, H. Vignolo-González, S. Schmidt, P. Mauker, T. Banerjee, P. Rovó, C. Ochsenfeld, B. V. Lotsch, *J. Am. Chem. Soc.* **2020**, *142*, 12146-12156.

[48] Y. Chen, D. Yang, B. Shi, W. Dai, H. Ren, K. An, Z. Zhou, Z. Zhao, W. Wang, Z. Jiang, *J. Mater. Chem. A* **2020**, *8*, 7724-7732.

[49] Q. Tang, Y.-Y. Gu, J. Ning, Y. Yan, L. Shi, M. Zhou, H. Wei, X. Ren, X. Li, J. Wang, C. Tang, L. Hao, J. Ye, *Chem. Eng. J.* **2023**, *470*, 144106.

[50] S.-Q. You, J. Zhou, M.-M. Chen, C.-Y. Sun, X.-J. Qi, A. Yousafa, X.-L. Wang, Z.-M. Su, *J. Catal.* **2020**, *392*, 49-55.

[51] G. Pan, X. Hou, Z. Liu, C. Yang, J. Long, G. Huang, J. Bi, Y. Yu, L. Li, *ACS Catal.* **2022**, *12*, 14911-14917.

[52] Z. Chen, J. Wang, M. Hao, Y. Xie, X. Liu, H. Yang, G. I. N. Waterhouse, X. Wang, S. Ma, *Nat. Commun.* **2023**, *14*, 1106.

[53] C. He, S. Tao, R. Liu, Y. Zhi, D. Jiang, *Angew Chem Int Ed Engl* **2024**, e202403472.

[54] Y. Chen, Q. Zhou, J. Zheng, *ACS Sustainable Chem. Eng.* **2022**, *10*, 1961-1971.

[55] a) M. Guo, Q. Meng, W. Chen, Z. Meng, M. L. Gao, Q. Li, X. Duan, H. L. Jiang, *Angew. Chem., Int. Ed.* **2023**, *62*, e202305212; b) W. Li, Z. Bie, C. Zhang, X. Xu, S. Wang, Y. Yang, Z. Zhang, X. Yang, K. H. Lim, Q. Wang, W. J. Wang, B. G. Li, P. Liu, *J. Am. Chem. Soc.* **2023**, *145*, 19283-19292.

[56] B.-J. Yao, J.-T. Li, N. Huang, J.-L. Kan, L. Qiao, L.-G. Ding, F. Li, Y.-B. Dong, *ACS Appl. Mater. Interfaces* **2018**, *10*, 20448-20457.

[57] a) Y. J. Chen, Y. Y. Wen, W. H. Li, Z. H. Fu, G. E. Wang, G. Xu, *Nano Lett.* **2023**, *23*, 3614-3622; b) M. Liu, Y. J. Chen, X. Huang, L. Z. Dong, M. Lu, C. Guo, D. Yuan, Y. Chen, G. Xu, S. L. Li, Y. Q. Lan, *Angew. Chem., Int. Ed.* **2022**, *61*, e202115308.

[58] a) L. Guo, S. Jia, C. S. Diercks, X. Yang, S. A. Alshmimri, O. M. Yaghi, *Angew. Chem., Int. Ed.* **2019**, *59*, 2023-2027; b) C. Liu, Z. Ye, X. Wei, S. Mao, *Electrochem. Sci. Adv.* **2021**, *2*, e2100137; c) X. Tang, Q. Zhang, D. Chen, L. Deng, Y. He, J. Wang, C. Pan, J. Tang, G. Yu, *Chem. Commun.* **2023**, *59*, 8731-8734.

[59] a) W. Gong, C. Liu, H. Shi, M. Yin, W. Li, Q. Song, Y. Dong, C. Zhang, *J. Mater. Chem. C* **2022**, *10*, 3553-3559; b) Y. Li, M. Chen, Y. Han, Y. Feng, Z. Zhang, B. Zhang, *Chem. Mater.* **2020**, *32*, 2532-2540; c) J.-L. Liang, Q.-N. Chen, J.-X. Zhang, W.-Q. Lian, Y.-X. Qiu, H.-Y. Xie, W.-T. Liu, W.-T. Xie, W.-Q. Xu, *Polyhedron* **2022**, *224*, 116014.

[60] W.-R. Cui, W. Jiang, C.-R. Zhang, R.-P. Liang, J. Liu, J.-D. Qiu, *ACS Sustainable Chem. Eng.* **2019**, *8*, 445-451.

[61] S.-Y. Ding, M. Dong, Y.-W. Wang, Y.-T. Chen, H.-Z. Wang, C.-Y. Su, W. Wang, *J. Am. Chem. Soc.* **2016**, *138*, 3031-3037.

[62] Y. Song, L. Guo, Y. Du, L. Yang, L. Wang, *Chem. Commun.* **2020**, *56*, 14913-14916.

[63] G. Chen, H.-H. Lan, S.-L. Cai, B. Sun, X.-L. Li, Z. He, S.-R. Zheng, J. Fan, Y. Liu, W.-G. Zhang, *ACS Appl. Mater. Interfaces* **2019**, *11*, 12830-12837.

[64] M. Xia, T. Shen, C. Li, R. Fan, L. F. b, Q. Chen, *Mate. Chem. Phys.* **2022**, *286*, 126208.

[65] D.-M. Li, S.-Y. Zhang, J.-Y. Wan, W.-Q. Zhang, Y.-L. Yan, X.-H. Tang, Sheng-Run Zheng, S.-L. Cai, W.-G. Zhang, *CrystEngComm* **2021**, *23*, 3594-3601.

[66] Y. Lu, Y. Liang, Y. Zhao, M. Xia, X. Liu, T. Shen, L. Feng, N. Yuan, Q. Chen, *ACS Appl. Mater. Interfaces* **2021**, *13*, 1644-1650.

[67] H. Singh, M. Devi, N. Jena, M. M. Iqbal, Y. Nailwal, A. D. Sarkar, S. K. Pal, *ACS Appl. Mater. Interfaces* **2020**, *12*, 13248-13255.

[68] J.-Y. Yue, L.-P. Song, Y.-T. Wang, P. Yang, Y. Ma, B. Tang, *Anal. Chem.* **2022**, *94*, 14419-14425.

[69] W. Ma, S. Jiang, W. Zhang, B. Xu, W. Tian, *Macromol. Rapid Commun.* **2020**, *41*, 2000003.

[70] S. Jiang, L. Meng, W. Ma, G. Pan, W. Zhang, Y. Zou, L. Liu, B. Xu, W. Tian, *Mate. Chem. Front.* **2021**, *5*, 4193-4201.

[71] Y. Zhang, X. Shen, X. Feng, H. Xia, Y. Mua, X. Liu, *Chem. Commun.* **2016**, *52*, 11088-11091.

[72] W. Gong, Y. Dong, C. Liu, H. Shi, M. Yin, W. Li, Q. Song, C. Zhang, *Dyes and Pigments* **2022**, *204*, 110464.

[73] H. Chen, H. Tu, C. Hu, Y. Liu, D. Dong, Y. Sun, Y. Dai, S. Wang, H. Qian, Z. Lin, L. Chen, *J. Am. Chem. Soc.* **2018**, *140*, 896-899.

[74] a) Q. Yang, X. Li, C. Xie, N. Liu, J. Yang, Z. Kong, Z. Kang, R. Wang, X. Li, D. Sun, *Nano Research* **2023**, *16*, 10946; b) J. Shuping, Z. Peng, Y. Yi, L. Qi, C. Yao, C. Peng, Z. Zhenjie, *Chem. Res. Chinese U.* **2022**, *38*, 461.

[75] X. Wu, Y.-l. Hong, B. Xu, Y. Nishiyama, W. Jiang, J. Zhu, G. Zhang, S. Kitagawa, S. Horike, *J. Am. Chem. Soc.* **2020**, *142*, 14357-14364.

[76] YanKong, X. He, H. Wu, YiYang, LiCao, R. Li, B. Shi, G. He, Y. Liu, Q. Peng, C. Fan, Z. Zhang, Z. Jiang, *Angew. Chem., Int. Ed.* **2021**, *60*, 17638-17646.

[77] X. Li, H. Wang, Z. Chen, H.-S. Xu, W. Yu, C. Liu, X. Wang, K. Zhang, K. Xie, K. P. Loh, *Adv. Mater.* **2019**, *31*, e1905879.

[78] S. Yao, Y. Yang, Z. Liang, J. Chen, J. Ding, F. Li, J. Liu, L. Xi, M. Zhu, J. Liu, *Adv. Funct. Mater.* **2023**, *33*, 2212466.

[79] K. Zhang, X. Li, L. Ma, F. Chen, Z. Chen, Y. Yuan, Y. Zhao, J. Yang, J. Liu, K. Xie, K. P. Loh, *ACS Nano* **2023**, *17*, 2901-2911.

[80] C. Yin, Z. Li, D. Zhao, J. Yang, Y. Zhang, Y. Du, Y. Wang, *ACS Nano* **2022**, *16*, 14178-14187.

10.1002/anie.202404941



WILEY VCH

REVIEW

## Entry for the Table of Contents

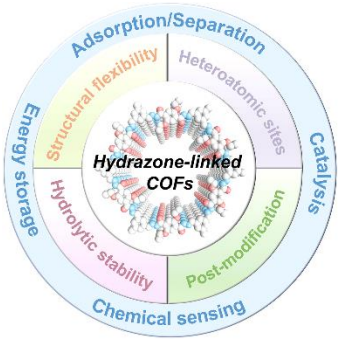


This review provides an introduction on the recent progresses made in the field of hydrazone-linked COFs for various applications including adsorption/separation, catalysis, chemical sensing and energy storage.